C.P. No. 1222

C.P. No. 1222

PROCUREMENT EXECUTIVE, MINISTRY OF DEFENCE

AERONAUTICAL RESEARCH COUNCIL

CURRENT PAPERS

Optimum Engine Thrust Deflection for High-Speed Cruising Aircraft

by

J. Pike

Aerodynamics Dept., R.A.E., Bedford

LONDON: HER MAJESTY'S STATIONERY OFFICE

1972

PRICE *70 p* NET

UDC 533.6.013.16 : 533.6.013.61 : 533.6.011.5 : 533.6.011.55 : 533.692.55

* CP.No.1222

June 1971

OPTIMUM ENGINE THRUST DEFLECTION FOR HIGH-SPEED CRUISING AIRCRAFT

by

J. Pike

SUMMARY

At high Mach numbers, an efficient cruising aircraft will have a significant fraction of its weight carried by the engines. At optimum conditions, the propulsive jet is inclined to the horizontal at an angle ϕ, given approximately by

$$\tan \phi \approx 1.06 \sqrt{C_w} - 1/(2.4\beta) \quad ,$$

where C_w is a nondimensionalised aircraft weight. At this angle, the net thrust required is about 20% less than the unvectored thrust. Also, compared with values from previous analysis at constant lift-to-drag ratio, the thrust deflection is approximately 50% larger, and the thrust required is typically 3% smaller.

---

* Replaces RAE Technical Report 71123 - ARC 33614

CONTENTS

1 INTRODUCTION

Consider an aircraft cruising in a homogeneous atmosphere at some fixed Mach number and height, with the lift and drag dependent on the aircraft's attitude. For constant Mach number, the drag is equal to the horizontal component of the engine thrust, and for constant height, the aircraft weight is equal to the sum of the lift and the vertical component of engine thrust. Thus, altering the engine thrust angle will require different lift, drag and thrust forces.

Previous studies of thrust deflection[1] have mainly assumed constant lift-to-drag ratio, or its equivalent. Here it is assumed that the variation in the lift-to-drag ratio with lift of the caret wing is typical of that of a lifting configuration for Mach numbers in the range where nozzle deflections are most significant ($M > 5$). Numerical optimisation studies using this assumption show that optimum nozzle deflection angles are commonly 50% larger than those suggested by analysis at constant lift-to-drag ratio. Further, the engine net thrust required is typically 20% less than the net thrust without deflection and typically 3% less than that suggested by analysis at constant lift-to-drag ratio. This decrease in the required thrust reduces the rate of fuel consumption, and thus increases the aircraft range or payload. Also the reduction in engine size and weight makes the problem of engine integration easier.

Under certain restricted conditions, analytical results are obtained for the optimum nozzle deflection angle, based on Newtonian, Busemann second order and linear theory relationships. They support the results obtained by numerical methods.

2 THE BASIC EQUATIONS

Consider a waverider aircraft of given weight with the propulsion system situated in the flow influenced by the lifting surface as shown in Fig.1 (see also Fig.14). For cruise conditions (strictly speaking at fixed altitude) the aircraft weight (W) is supported by the aerodynamic lift, the vertical component of engine thrust and the centrifugal force due to the earth's curvature. As the velocity of the aircraft is constant, we consider throughout an apparent weight ($\overline{W}$) which includes the centrifugal force term, i.e.

$$\overline{W} = W\left(1 - \frac{V_\infty^2}{V_s^2}\right) \qquad (1$$

where V_∞ is the aircraft velocity and V_s is the equivalent satellite orbital speed. In Fig.2 the apparent weight as a fraction of the (gravity)

weight is shown. Up to about Mach 8 the apparent weight differs from the actual weight by less than 10%; at higher Mach numbers a greater fraction of the weight is carried by centrifugal effects.

Vertical resolution of the forces on the aircraft (see Fig.1) gives

$$L + T_2 \sin \phi - T_1 \sin \delta = \bar{W} \tag{2}$$

where L is the lift, T_1 is the reaction pressure* of the intake and T_2 is the reaction pressure of the engines in the nozzle exit plane. A more detailed discussion of these parameters is given in Appendix A. Non-dimensionalising equation (2) with respect to planform area (S) and dynamic pressure (q_∞) we obtain

$$C_L + C_{T2} \sin \phi - C_{T1} \sin \delta = C_W = \frac{\bar{W}}{q_\infty S} \quad . \tag{3}$$

For the cruise condition assumed, C_W is a constant and the horizontal component of engine thrust exactly balances the drag, i.e.

$$C_{T2} \cos \phi - C_{T1} \cos \delta = C_D \quad . \tag{4}$$

Then the following basic equations are obtained by eliminating ϕ and C_{T2} respectively from equations (3) and (4):-

$$C_{T2}^2 = (C_W - C_L + C_{T1} \sin \delta)^2 + (C_D + C_{T1} \cos \delta)^2 \tag{5}$$

$$\tan \phi = \frac{C_W - C_L + C_{T1} \sin \delta}{C_D + C_{T1} \cos \delta} \quad . \tag{6}$$

To find the value of ϕ which minimises the engine thrust $(C_T = C_{T2} - C_{T1})$, the right hand sides of equations (5) and (6) are expressed as functions of a single variable (C_L). The engine thrust is then minimised with respect to C_L by use of equation (5), and optimum values of ϕ are evaluated using equation (6). It should be noted that if L/D is constant, optimum ϕ from equations (5) and (6) is given by $\phi = \cot^{-1} (L/D)$, as has been found previously[1].

---

* The reaction pressure is the sum of the static and momentum pressures.

In the next section a preliminary investigation is undertaken for nearly-delta planforms, by expressing C_D and δ as functions of C_L using Newtonian, Busemann second order, and linear theories. In section 4 caret wing values are used, and a complete set of results is obtained using numerical optimisation.

3 A SIMPLE EXAMPLE FOR RESTRICTED CONDITIONS

To express C_D, C_{T1} and δ as functions of C_L, it is necessary to make assumptions concerning the aerodynamics of the aircraft. Suppose we assume that the incidence $\delta \ll 1$ radian and the planform is nearly delta; then the lift coefficient is given approximately by

$$C_L = A\delta + B\delta^2 + O(\delta^3) \quad . \tag{7}$$

For low supersonic Mach numbers, linear theory gives $A = 4/\beta$, $B = 0$. For very high Mach numbers, Newtonian theory gives $A = 0$, $B = 2$. For moderate Mach numbers we use a Busemann second order expression where $A = 2/\beta$ and $B = (\gamma + 1)/2$. We also assume that C_{T1} is constant and large compared with the drag. These assumptions, and the $\delta \ll 1$ restriction, are introduced for analytical reasons. Physically they are crude assumptions requiring that the precompression of the intake air by the lifting surface is constant, and that enough air of high Mach number is swallowed by the intake for its reaction pressure to be much greater than the drag. The precompression across the shock wave of a caret wing at various values of $\cot \delta$ and C_L is shown in Fig.3. We see that the variation of p/p_∞ with δ is smaller for high lift-to-drag ratio, but that it could still be significant.

Substituting for C_L from equation (7) in equation (5), we obtain

$$C_{T2}^2 = (C_w - A\delta - B\delta^2 + C_{T1} \sin \delta)^2 + (C_{DF} + (A\delta + B\delta^2) \tan \delta + C_{T1} \cos \delta)^2 \quad . \tag{8}$$

As C_{T1} is constant, minimum engine thrust is given by minimum C_{T2}. Hence differentiating equation (8) with respect to δ and putting $dC_{T2}/d\delta = 0$ gives

$$(C_w - C_L + C_{T1} \sin \delta)(C_{T1} \cos \delta - A - 2B\delta)$$
$$+ (C_D + C_{T1} \cos \delta)(C_L \sec^2 \delta + \tan \delta \, (A + 2B\delta) - C_{T1} \sin \delta) = 0 \quad . \tag{9}$$

With $\delta \ll 1$ and $C_D \ll C_{T1}$, this reduces to

$$(C_w - C_L)(C_{T1} - A - 2B\delta) = - C_{T1}C_L \quad . \tag{10}$$

From equation (7) we have

$$A + 2B\delta = (A^2 + 4BC_L)^{\frac{1}{2}} \tag{11}$$

hence equation (10) can be written

$$\frac{C_w - C_L}{C_w} = \frac{C_{T1}}{(A^2 + 4BC_L)^{\frac{1}{2}}} \quad . \tag{12}$$

Thus we have the contribution of engine thrust to the total lift porportional to the intake reaction. Further, using linear theory values for A and B, we have that the thrust contribution is proportional to β. However this increase with Mach number only applies at low Mach number, for Newtonian theory suggests that the thrust contribution is given by $C_{T1}/\sqrt{8C_L}$.

From equation (6)

$$\tan \phi = \frac{C_w - C_L}{C_{T1}} + \delta \quad . \tag{13}$$

For values of $(C_w - C_L)$ and δ derived from linear theory, this expression becomes

$$\tan \phi = \frac{\beta C_W}{4}\left(1 - \frac{\beta C_{T1}}{4}\right) \quad . \tag{14}$$

For $B \neq 0$, equations (11), (12) and (13) give

$$\tan \phi = \frac{C_w}{(A^2 + 4BC_L)^{\frac{1}{2}}} + \frac{(A^2 + 4BC_L)^{\frac{1}{2}}}{2B} - \frac{A}{2B}$$

$$= \frac{3}{2}\left(\frac{C_w}{B}\right)^{\frac{1}{2}} \frac{1 - \frac{2}{3}\frac{C_w - C_L}{C_w} + \frac{A^2}{6BC_w}}{\left\{1 - \frac{C_w - C_L}{C_w} + \frac{A^2}{4BC_w}\right\}^{\frac{1}{2}}} - \frac{A}{2B} \quad . \tag{15}$$

For $\frac{C_w - C_L}{C_w} - \frac{A^2}{4BC_w} < \frac{1}{2}$ we have

$$\tan \phi \sim \frac{3}{2}\left(\frac{C_w}{B}\right)^{\frac{1}{2}} - \frac{A}{2B} \cdot \tag{16}$$

Hence the Newtonian values for A and B give

$$\tan \phi = 1.06 \sqrt{C_w} \quad \text{for} \quad C_L > C_w/2 \tag{17}$$

(that is when the aerodynamic lift carries at least half of the weight), and the Busemann second order assumption gives

$$\tan \phi = \frac{3}{2}\left(\frac{2C_w}{\gamma + 1}\right)^{\frac{1}{2}} - \frac{1}{(\gamma + 1)\beta} \tag{18}$$

for

$$C_L + \frac{8}{(\gamma + 1)\beta^2} > \frac{C_w}{2}$$

(that is except when the aerodynamic lift carries rather more than half the weight).

Equations (14), (17) and (18) are 'patched' over their regions of most applicability in Fig.4. The poor matching along the line $\beta^2 C_w = \frac{1}{2}$ (shown dotted), is due to the step change in the value of A between the linear theory value which includes upper surface lift, and the Busemann value which assumes it is small. The spread of the linear theory curves represents a range of C_{T1}, (a range of $0 \leqslant C_{T1} \leqslant 1/M$ is used, and this is discussed later). This contrasts with the Busemann and Newtonian curves which do not show any variation in ϕ with C_{T1}. Equations (16) and (17) suggest that ϕ does not vary with aerodynamic drag either, and that its variation with $\sqrt{C_w}$ is linear. From Fig.4, it can be seen that linear theory is only used over a region where the optimum nozzle deflection is small. If we exclude this region of low Mach number and lift coefficient (strictly where $\beta C_L^2 < 0.55$), we find that not only in the restricted case dealt with in this section, but also for the more complete case of the following section, ϕ can be represented as a simple function of C_w and Mach number only.

4 A COMPLETE ANALYSIS FOR THE CARET WING

At high Mach numbers where the upper surface lift tends to be less important, we take the caret wing* to be typical of waverider wings[2]. The pressure drag and surface angle (δ): are given by[3]

$$C_{DP} = C_L \tan\delta = \frac{C_L^2}{2 - C_L}\left\{\frac{M^2 - 1 - (\gamma + 1)C_L M^2/4}{1 + (\gamma + 1)C_L M^2/4}\right\}^{\frac{1}{2}} \tag{19}$$

For $3 < M < 6$ and $C_L < 0.2$ the viscous drag of an inclined flat plate can be represented approximately by[3]

$$C_{DF} = C_{DFO} + C_{DF1}C_L \tag{20}$$

where C_{DFO} and C_{DF1} are constants. At hypersonic Mach numbers it has been shown[4] that friction drag varies as $1/M_1^2$, where M_1 is the Mach number at the edge of the boundary layer. For the caret wing from oblique shock wave relationships, we have

$$\frac{1}{M_1^2} = \left(\frac{1}{M^2} + \frac{\gamma - 1}{4} C_L\right) K \tag{21}$$

where $\frac{1}{K} = 1 - C_L \dfrac{1 + M^2(\gamma - 1 + \gamma^2 C_L)/4}{1 + M^2\gamma C_L/2}$.

For $C_L < 0.2$, K is near unity. Hence the relationship of equation (20) also applies approximately for hypersonic Mach numbers. Equation (20) is used here as a first approximation to the variation of friction drag with lift coefficient. For lifting configurations C_{DFO} is the friction drag at zero lift, and C_{DF1} is a correction factor to allow for the higher friction drag at incidence.

From equations (19) and (20) the total drag C_D (i.e. $C_{DP} + C_{DF}$) can be expressed as a function of C_L. To obtain C_{T1} as a function of C_L it is assumed that the mass of air captured by the intake is constant, that is, the area (A_p) of the free stream tube of air which will be captured by the intake is constant. Thus

---

* The caret wing has a delta planform, pronounced anhedral and supports a plane oblique shock wave at design incidence and M_∞.

$$C_{T1} = \frac{T_1}{q_\infty S} = \frac{\rho_\infty V_\infty V_1 A_p}{q_\infty S} = \frac{2A_p}{S}\frac{V_1}{V_\infty}$$

where V_1 is the velocity just upstream of the intake.

Evaluating V_1/V_∞ from caret wing conditions gives

$$C_{T1} = \frac{2A_p}{S}\left(1 - C_L \frac{4 + \gamma C_L M^2}{4 + (\gamma + 1)C_L M^2}\right) \quad . \tag{22}$$

Hence from equations (5), (6), (19), (20) and (22), C_T and $\tan\phi$ may be expressed as functions of C_L, M, C_w and A_p/S, i.e.

$$C_T = C_{T2} - C_{T1} = \left\{\left[C_w - C_L + \frac{2A_p}{S}\left(1 - C_L \frac{4 + \gamma C_L M^2}{4 + (\gamma + 1)C_L M^2}\right)\cos\delta\right]^2 + \left[C_{DFO} + C_{DF1}C_L + C_L \tan\delta + \frac{2A_p}{S}\left(1 - C_L \frac{4 + \gamma C_L M^2}{4 + (\gamma + 1)C_L M^2}\right)\cos\delta\right]^2\right\}^{\frac{1}{2}} - C_{T1} \tag{23}$$

and

$$\tan\phi = \frac{C_w - C_L + 2\sin\delta \frac{A_p}{S}\left(1 - C_L \frac{4 + \gamma C_L M^2}{4 + (\gamma + 1)C_L M^2}\right)}{C_{DFO} + C_{DF1}C_L + C_L \tan\delta + 2\cos\delta \frac{A_p}{S}\left(1 - C_L \frac{4 + \gamma C_L M^2}{4 + (\gamma + 1)C_L M^2}\right)} \tag{24}$$

where $\tan\delta = \frac{C_L}{2 - C_L}\left(\frac{4M^2 - 4 - (\gamma + 1)C_L M^2}{4 + (\gamma + 1)C_L M^2}\right)^{\frac{1}{2}}$.

For given cruise conditions, C_T and $\tan\phi$ can be calculated for any C_L. In Fig.5, the variation of C_T/C_w (i.e. thrust/apparent weight) with $\tan\phi$ is shown for $C_w = 0.05$, 0.1 and 0.15, $C_{DF} = 0.002$, $A_p/S = 0.04$ and Mach numbers of 5 and 10. Typically, for a wing loading of 75 lb/sq ft and a temperature of 800 K at 5 ft behind the leading edge at M = 5, the cruising height is 95000 ft [5] and $C_w = 0.16$, similarly at M = 10, 1200 K and 130 000 ft, C_w is also equal to 0.16 so that values of C_w in the range 0 to 0.2 are appropriate. It should be noted that with thrust deflection, some of the wing loading quoted above is carried by the engines and the lift loading

will then be different from the wing loading. The weight per unit area is probably more significant for structural use, while the lift per unit area is important for wing heating and boundary layer development. Thus it may be important to distinguish between them when thrust deflection is used.

In Fig.5 for the values of C_w indicated, we see that inclining the nozzle can reduce the thrust required by up to 20%. The deflections predicted if lift-to-drag ratio is assumed to be constant are shown by the dotted line. These considerably under-estimate the deflection angle for minimum thrust, and require that the thrust be about 3% greater than the minimum shown.

The thrust-to-weight ratio obtained in Fig.5, falls with decreasing weight coefficient, suggesting that efficient vehicles may need low wing loadings. Note that small changes in ϕ from the values for minimum thrust cause insignificant changes in the required thrust.

Minimum values of C_T, with the associated ϕ and C_L values, have been obtained numerically from equations (23) and (24), with a maximum allowed error in C_L of 0.2% of C_w. The details of the method are given in Appendix B.

The results obtained with free stream Mach numbers of 5, 7 and 10 and several values of C_{DF} are presented in Figs.6 to 11. Figs.6 to 8 show the effects of Mach number changing with a constant friction drag (i.e. $C_{DF} = 0.002$). Figs.8 to 10 show the effects of increase in friction drag for a constant Mach number (i.e. M = 10), and Fig.11 shows the results for a friction drag which varies with lift coefficient (i.e. $C_{DF} = 0.002\ (1 + 10C_L)$ from equation (20) and Ref.3 for $M = 10$ and $\gamma = 1.4$).

Figs.6 to 11 each show four plots labelled (a) to (d), which have C_w as abscissa and, as ordinates, the ratio of aerodynamic lift to the apparent weight (C_L/C_w), thrust to apparent weight $(T/\bar{W})$, thrust deflection angle (ϕ), and the ratio of thrust deflection to that for constant lift-to-drag ratio conditions $((L/D) \tan \phi)$. The five curves on each plot represent five values of the free stream capture area of the intake (i.e. $A_p/S = 0$, 0.1/M, 0.4/M, 0.7/M and 1/M). Note that in some cases the curves for 0 and 0.1/M are so close as to be indistinguishable and only four curves are plotted. At the largest value of the intake airflow (i.e. $A_p/S = 1/M$), a major portion of the air affected by the lifting compression surface is swallowed by the intake. It should be noted that as engine efficiency must be expected to be strongly dependent on A_p/S, comparison between the five curves should be made with caution.

A wide range of C_w and A_p/S (i.e. $0 \leqslant C_w \leqslant 0.2$, $0 \leqslant A_p/S \leqslant 1/M$) is shown on each of the plots. Typical practical values for these parameters can be obtained from design studies of hypersonic transports. For example, a design study for a Mach 7 kerosene-burning transport[6] yielded a configuration which at the start of its cruise flight at 100 000 ft had $A_p/S \sim 0.04$, $C_w \sim 0.07$ and $C_D \sim 0.009$. Most of the drag was lift-dependent drag, the zero lift drag coefficient (C_{DF}) being about 0.002. In Ref.7 it is suggested that A_p/S varies approximately as $1/M^2$, and that at Mach 10 it has a value of about 0.06. Two typical values from the results of Ref.9 are shown in Figs.7 and 8 by the 'diamond' shaped symbols. These values are for configuration with optimised 3 shock wave intakes, a maximum temperature in the engine of 8 times free stream temperature and no thrust deflection. We see that for these examples $A_p/S \sim 0.07$, and $C_w = 0.045$ at $M = 10$ and 0.08 at $M = 7$. Thus, in general, the regions of most practical interest probably occur at rather less than the median values of the parameters shown.

Of the plots shown in Figs.6 to 11, plots (a) show the proportions of weight carried by the pressure under the wing (i.e. C_L/C_w) and by the engine (i.e. $1 - C_L/C_w$). When $A_p/S = 0.1/M$, the vertical component of engine thrust is about 8-10% of the weight. As the amount of air used by the engines increases, so does the proportion of weight carried by the engine thrust, as was suggested by the example of section 3. Linear theory further suggests that the fraction of weight which ought to be carried by the engine thrust increases with Mach number. However, Figs.6a, 7a and 8a show a slight tendency for $(1 - C_L/C_w)$ to fall with Mach number, a result closer to that suggested by Newtonian theory.

C_L/C_w also represents the ratio of the lift loading to the wing loading. Thus when $A_p/S = 0.1/M$ the lift loading is only about 90% of the wing loading and the aerodynamic heating and friction drag will be less than with the unvectored thrust configuration. Consider an example based on Fig.11, where $C_{DF} = 0.002\ (1 + 10C_L)$. If $C_L = 0.05$ and $A_p/S = 0.4/M$, then $C_{DF} = 0.003$ and $C_L/C_w = 0.8$ from Fig.11a. Hence $C_w = 0.0625$ and C_{DF} for the unvectored thrust configuration would be 0.00325, an increase of about 8% in friction drag. The increase in thrust required to overcome this extra drag would of course be in addition to that already demonstrated for the unvectored thrust.

For $A_p/S = 1/M$ and small values of C_w, nearly all the weight is carried by the engines and the aerodynamic lift can be neglected. Equations (5) and (6) then become simply

$$C_{T2}^2 = C_2^2 + (C_{T1} + C_{DF})^2 \qquad (25)$$

and

$$\tan \phi = C_w/(C_{T1} + C_{DF}) \quad . \qquad (26)$$

This result is similar to that at constant lift-to-drag ratio, where the lift is replaced by the weight and the drag includes the intake reaction. We note, however, that for most of the range of interest both the aerodynamic and the engine lift are important.

The aim of deflecting the thrust T_2 is to reduce the required net thrust T (i.e. $T_2 - T_1$). Plots (b) show minimum values of the ratio of thrust to apparent weight (i.e. $T/\bar{W}$ or $(C_{T2} - C_{T1})/C_w$) for C_w up to 0.2. It can be seen that $T/\bar{W}$ is smallest for C_w values of about 0.04 or 0.05. The minimum value of $T/\bar{W}$ increases with Mach number and C_{DF}, from about 0.1 when $M = 5$ and $C_{DF} = 0.002$, to about 0.2 when $M = 10$ and $C_{DF} = 0.004$.

Analysis relating to lifting configurations without a propulsion system, suggests that, for high aerodynamic efficiency the friction drag should be slightly less than the pressure drag[3,8]. It is interesting to consider the ratio of friction drag to total drag for the configurations obtained here. In Fig.12, where this is plotted, there is considerable variation in the ratio. However when the ratio of friction to total drag is 0.4 (giving good aerodynamic efficiency), we find significantly, that the thrust-to-weight ratio in plots (b) is near its minimum value, with the exception of those cases where most of the weight is supported by the engines.

Unless low wing loadings and high surface temperatures[5] are acceptable values of C_w much larger than 0.05 are required. Thus a compromise will exist between the values of C_w for minimum thrust suggested here and structural requirements. As the thrust penalty for moving away from the minimum is at first small, practical values of C_w must be expected to be greater than the value for minimum $T/\bar{W}$. For the hypersonic transport of Ref.6, the value of C_w was 0.07. For values of C_w above about 0.06, $T/\bar{W}$ increases nearly linearly with C_w, such that with $C_{DF} = 0.002$ for the range of M and C_w a 1% increase in weight requires a 2% increase in thrust. This penalty for weight

increase, may demand that, for a cruising aircraft, the value of C_w is not too remote from the minimum thrust value. It is clear that improvements in materials or structural design which lighten the airframe, will produce significant increases in the efficiency of hypersonic cruising aircraft.

The thrust deflection angle is shown plotted against C_w in plots (c). Equations (17) and (18) of section 3 suggest a simple variation of ϕ with C_w and Mach number. In Fig.13, the results shown in Figs.6-11c are plotted according to a relationship indicated in equation (18); that is for $\gamma = 1.4$ they are plotted as $\tan \phi + 1/2.4\beta$ against $\sqrt{C_w}$. We see that for a wide range of engine mass flow, friction drag and Mach number, all the curves collapse closely on to the line obtained from Newtonian theory (equation (17)), and indicated in Fig.13 by the 'arrows'. Hence for $M \geqslant 5$ and $C_w > 0.01$, ϕ is given by the simple relationship

$$\tan \phi \approx 1.06 \sqrt{C_w} - 1/2.4\beta \quad . \tag{27}$$

Thus the optimum thrust deflection angle may be obtained directly from the aircraft weight, plan area and cruise conditions.

The aircraft weight varies throughout the cruise phase of the flight as the fuel is used. Equation (27) thus suggests that for fixed height the thrust inclination should decrease during the flight. However if the cruise height increases during the flight such that ρ_∞ decreases as the weight, C_w and thus ϕ will be constant.

Although the present analysis is based on aircraft weight, the angle which would have been suggested by assuming constant lift-to-drag ratio (i.e. $\delta = \cot^{-1} (L/D)$) can be evaluated for the particular configurations obtained. In plots (d), the ratio of the tangents of the two angles (i.e. $(L/D) \tan \phi$) is shown. For the range of C_w (or C_L) of practical interest, we see that ϕ is substantially larger than $\cot^{-1} (L/D)$. Thus at a given altitude, adopting the angle based on constant lift-to-drag ratio would result not only in higher thrust, but also larger lift loading, giving greater aerodynamic heating and friction drag.

It should be noted that although for simplicity the results are derived for constant height and speed, they apply also for constant rates of change of speed and a climb angle θ, if the weight coefficient C_w is replaced by $C_w \cos \theta$ and C_{DFO} is replaced by $(C_{DFO} + C_w \sin \theta + (C_w \dot{v}/g))$ throughout.

5 CONCLUSIONS

When the engine thrust is deflected so as to minimise net thrust, it is found for $M \geqslant 5$, that the thrust may support a significant proportion of the aircraft weight. For example, when the engine air free stream tube is about $0.1/M$ of the plan area, the thrust supports about 10% of the weight. This percentage increases rapidly with increasing engine free stream capture area, until for certain conditions nearly all the lift is provided by the engines.

The minimum thrust to weight ratio varies markedly with weight coefficient $(\bar{W}/q_\infty S)$. Its smallest value occurs at a weight coefficient of 0.04, which is thought to be rather low for practical purposes. The value of the thrust-to-weight ratio is then about 0.1 for $M = 5$ and $C_{DF} = 0.002$, and increases with Mach number and friction drag to about 0.2 when $M = 10$ and $C_{DF} = 0.004$. These values occur near the conditions of maximum lift-to-drag ratio of the lifting surface.

In practice, there is a tendency for structural requirements to require weight coefficients larger than the values for minimum thrust-to-weight ratio. At these higher values of weight coefficient, the minimum thrust-to-weight ratio increases almost linearly with weight coefficient, such that typically for $C_{DF} = 0.002$ a 1% increase in weight requires a 2% increase in thrust. Hence, for a cruising aircraft, there is a considerable extra incentive for keeping the structure weight as low as possible.

It is found that the thrust deflection for minimum thrust is almost independent of friction drag and engine free stream capture area. A simple but accurate expression for the optimum inclination to the horizontal of the cruising thrust is given by

$$\tan \phi \approx 1.06 \sqrt{C_w} - 1/2.4\beta \quad .$$

The adoption of this angle for a cruising aircraft results in a thrust requirement typically 20% less than the unvectored thrust and 3% less than the value from analysis at constant lift-to-drag ratio. A further advantage of thrust deflection is that, for a given weight coefficient, the aerodynamic loading of the lifting surface is reduced, thus reducing the aerodynamic heating and skin friction.

Appendix A

DEFINITION OF AERODYNAMIC AND PROPULSIVE FORCES

At hypersonic Mach numbers the division of the forces on an aircraft into 'propulsive' and 'aerodynamic' forces is, to some extent, arbitrary. For example, forces associated with the intake pre-entry flow, the flow over the engine cowl and the influence of the engine cowl on the wing, do not conveniently fit into either category. It may be argued that analysis which requires that all these forces necessarily be grouped as aerodynamic or propulsive will be artificial, and worthwhile results can best be obtained from project analysis for particular configurations. However from a limited number of project results, it is difficult to establish general relationships between the parameters involved. General relationships, if they exist, are not only more likely to be found from analysis admitting a range of configurations but are often largely independent of the detailed assumptions necessary to define the problem. For example, it is found in this Report that the results based on the crude assumptions of section 3, predict remarkably closely the main results based on the more detailed assumptions of section 4.

The relationships of particular interest in the Report, are those between the engine thrust deflection and the aerodynamic parameters of the aircraft. In Fig.14a, an aircraft configuration without a propulsion system is shown. The approximate aerodynamic force coefficients of such wings have been postulated[2,8] for a wide range of hypersonic Mach numbers and lift coefficients. Hence these wings provide a convenient aerodynamic basis for analysis. In Fig.14b a propulsion system has been added and five components included here in the propulsive force are listed.

The reaction pressure (i.e. the static and momentum pressures) integrated over the intake (see (i) of Fig.14b) is denoted by T_1 in the Report. If the flow approaching the intake is not uniform, T_1 will differ slightly according to the surface of integration used. For intakes which start their compression with a shock wave, this surface is most conveniently taken just upstream of the shock wave. If the intake compression is initially isentropic, distinguishing the lifting surface compression from the intake compression may be more difficult. A convenient surface to define uniquely the intake reaction in this case, is the upstream Mach surface from the cowl lip. The effect of small changes in the wing surface downstream of the intersection of this Mach surface with the wing are swallowed by the intake and will not affect the

lifting flow. Examples of these surfaces are shown in Fig.14c. In the left hand section the dashed line at the intake shows a typical surface[9] just upstream of the shock wave. The right hand section shows a typical surface for an isentropic compression.

The reaction pressure at the nozzle and any interference effects of the jet or cowl on the flow are included with the nozzle thrust term (T_2). For example, expansion of the jet downstream of the cowl may be used to provide considerable additional force on an appropriately reshaped wing. This force (minus that which would have been obtained from the same region of the clean configuration), is included in the thrust term T_2 (see (iv) of Fig.14). The engine cowl can have pressure forces on it differing from those of the clean wing, and can also influence the pressure over a region of the wing (see (ii) and (v) of Fig.14). These forces are also included in the thrust term T_2.

Friction forces differ for the two wings due to different surface curvatures and wetted areas, but as these forces are dealt with rather crudely by assuming an overall skin friction drag, this is taken to relate to the drag of the configuration with its propulsion system.

Appendix B

THE COMPUTER PROGRAM

The results of section 4 were obtained using the computer program shown below. It is written in Algol 60, with programming restrictions and input-output conventions suitable for an Elliott 503 digital computer.

```
J. Pike, HSST, RAE Bedford, Sept. 67
Optimum Nozzle deflection for Waveriders;
begin
real  g,M,SioS,CW,CDFO,CDFI,CPLmin,CTmin,delmin,CTImin,zeta;
Boolean premi;
switch ss:=AA;
real procedure CTI(P);value P; real P;
begin CTI:=2*sqrt(1-P*(1+g/4*M*M*P)/(1+(g+1)/4*M*M*P))*SioS;
end CTI;
real procedure del(P); value P; real P;
begin del:=arctan(P/(2-P)*sqrt((M*M-1-(g+1)/4*M*M*P)/(1+(g+1)/4*M*M*P)));
end del;
real procedure CT(P); value P; real P;
begin CT:=sqrt((CW-P+CTI(P)*sin(del(P)))↑2+(CDFO+CDFI*P+P*sin(del(P))/cos(del(P))+
      CTI(P)*cos(del(P)))↑2)-CTI(P);
end CT;
real procedure Fibonacci search (a,b,eps,fval,prem);
value a,b,eps; real a,b,eps,fval;
Boolean prem;
begin
real e,ff1,ff2,p1,p2;
integer n,f1,f2,c; Boolean equal;
switch sss:=EXIT;
equal:=false;
n:=1;f1:=2;f2:=3;
e:=(b-a)/eps;
for c:=f1 while f2<e do
begin n:=n+1;f1:=f2;f2:=c+f2
end;
p2:=(f1/f2)*(b-a)+a;p1:=a+b-p2;
ff1:=CT(p1);ff2:=CT(p2);
```

```
for n:=n step -1 until 2 do
begin c:=f1;f1:=f2-f1;f2:=c;
      if ff2≥ff1 then
      begin b:=p2;p2:=p1;
      p1:=checkr(b-(f1/f2)*(b-a));
      ff2:=ff1;ff1:=checkr(CT(p1))
               end else
      begin a:=p1;p1:=p2;
            p2:=a+(f1/f2)*(b-a);
            ff1:=ff2;ff2:=CT(p2)
      end;
      prem:=equal1 and ff1=ff2;
      if prem then goto EXIT;
      equal:=ff1=ff2
end;
EXIT :if ff2<ff1 then
begin fval:=ff2; Fibonacci search:=p2
end else
begin fval:=ff1; Fibonacci search:=p1
end
end Fibonacci search;
print £ Output in order g,M,CW,SioS,CDFO,CDFI,CTmin,CTImin,CTImin*Beta,CPLmin,
CPLmin/CW,zeta,delmin,tan(zeta)/tan(delmin),Ap/A?;
AA: read g,M,CDFO,CDFI:
for CW:-0.01 step 0.01 until 0.2 do
for SioS:=0.1/M step 0.3/M until 1/M+0.001 do
begin CPLmin:=Fibonacci search (0,CW,CW/500,CTmin,premi);
      delmin:=del(CPLmin);
      CTImin:=CTI(CPLmin);
      zeta:=arctan((CW-CPLmin+CTImin*sin(delmin))/(CDFO+CDFI*CPLmin+CPLmin*sin
      (delmin)/cos(delmin)+CTImin*cos(delmin)))-delmin;
      print aligned(2,5),g,sameline,M,CW,SioS,CDFO,CDFI,ff1??,CTmin,CTImin,
            CTImin*sqrt(M*M-1),CPLmin,CPLmin/CW,zeta*180/3.14159,delmin*180/3.14159,
            cos(delmin)/cos(zeta)*sin(zeta)/sin(delmin),SioS*(2-CPLmin)/CPLmin*
            sin(delmin)/cos(delmin),ff12??;
      if premi then print £ accuracy uncertain £12??;
end; go to AA;
end;
```

The optimisation procedure 'Fibonacci search' finds the value of the minimum of a function in an interval (a,b). It is used to find the lift coefficient which minimises C_T in equation (23). The input parameters are γ, M, C_{DFO} and C_{DFI}, giving an output at intervals of 0.1 in C_w and 0.3/M in A_p/S (NB SioS is used as the program symbol for A_p/S).

A sample of the input and output is shown below. On the upper line for each case are given the parameters γ, M, C_w, A_p/S, C_{DFO} and C_{DFI}. On the line below are printed consecutively the minimum value of the thrust ($C_{T\ min}$) and associated values of input reaction, $\beta \times$ input reaction, C_L, C_L/C_w, $\phi - \delta$, δ, $\tan(\phi - \delta)/\tan(\delta)$ and the fraction of the total air influenced by the caret wing compression surface in the base plane which has been swallowed by the intake. If the program is unable to obtain a 0.2% accuracy in C_L, the caption 'accuracy uncertain' is printed after the case where the failure has occurred.

Data

1.4, 10, 0.002, 0

Results

Output in order g,M,CW,SioS,CDFO,CDFI,CTmin,CTImin,CTImin*Beta,CPLmin,CPLmin/CW, zeta,delmin,tan(zeta)/tan(delmin),Ap/A.

1.40000 10.00000 0.01000 0.01000 0.00200 0.00000
0.00238 0.01992 0.19822 0.00920 0.91967 1.84193 2.10726 0.87400 0.07965

1.40000 10.00000 0.01000 0.04000 0.00200 0.00000
0.00234 0.07975 0.79352 0.00707 0.70656 2.00204 1.68963 1.18504 0.33281

1.40000 10.00000 0.01000 0.07000 0.00200 0.00000
0.00230 0.13972 1.39020 0.00438 0.43770 2.25229 1.11116 2.02777 0.61902

1.40000 10.00000 0.01000 0.10000 0.00200 0.00000
0.00225 0.19999 1.98991 0.00007 0.00656 2.81542 0.01865 1.51_{10}+02 0.99302

1.40000 10.00000 0.02000 0.01000 0.00200 0.00000
0.00330 0.01985 0.19754 0.01866 0.93279 2.81600 3.66127 0.76870 0.06796

1.40000 10.00000 0.02000 0.04000 0.00200 0.00000
0.00322 0.07951 0.79107 0.01541 0.77049 3.06626 3.17261 0.96641 0.28554

1.40000 10.00000 0.02000 0.07000 0.00200 0.00000
0.00313 0.13934 1.38745 0.01125 0.56230 3.47610 2.48097 1.40195 0.53636

1.40000 10.00000 0.02000 0.10000 0.00200 0.00000
0.00299 0.19972 1.98716 0.00302 0.15082 4.79772 0.79160 6.07459 0.91474

etc.

PRINCIPAL SYMBOLS

C_D	drag coefficient (D/Sq_∞)
C_{DF}	friction drag coefficient based on plan area
C_{DP}	pressure drag coefficient (D_p/Sq_∞)
C_L	lift coefficient (L/Sq_∞)
C_{T1}	intake reaction coefficient (T_1/Sq_∞)
C_{T2}	nozzle reaction coefficient (T_2/Sq_∞)
C_T	engine thrust coefficient $(C_{T2} - C_{T1})$
C_w	weight coefficient $(\bar{W}/Sq_\infty)$
D	drag
L	lift
S	plan area
T_1	thrust associated with intake air, i.e. reaction pressure integrated over intake entry
T_2	thrust associated with nozzle air, i.e. reaction pressure integrated over nozzle exit plane
W	aircraft weight
$\bar{W}$	apparent aircraft weight in flight (i.e. W - centrifugal force)
β	$(M^2 - 1)^{\frac{1}{2}}$
δ	angle intake flow makes with free stream direction
ϕ	angle nozzle reaction vector makes with free stream direction

REFERENCES

No.	Author(s)	Title, etc.
1	S.L. Bragg	Flight efficiency of air-breathing engines. Aeronautical Quarterly, Vol.14, pp.221-233 (1963)
2	D. Küchemann	Hypersonic aircraft and their aerodynamic problems. Progress in Aeronautical Sciences Vol.6 (1965)
3	J. Pike	On lifting surfaces supporting one or more plane shock waves. ARC R & M 3623 (1970)
4	D.E. Coles	The turbulent boundary layer in a compressible fluid. Rand R-403-PR (ARC 24497), September 1962
5	A. Naysmith J.G. Woodley	Equilibrium temperatures on lifting surfaces at Mach numbers between 5 and 12 at altitudes from 80000 ft up to 150 000 ft. RAE Technical Report 67114 (ARC 29851) (1967)
6	G.J. Pietrangeli E.V. Nice	The feasibility of a Mach 7 transport employing air-breathing propulsion systems. USA Johns Hopkins University APL-CF-2900, November 1960
7	D. Küchemann	An analysis of some performance aspects of various types of aircraft designed to fly over different ranges of different speeds. Progress in Aeronautical Sciences, Vol.9, pp.329-456 (1968)
8	J. Pike	On the maximum lift to drag ratio of wings at high Mach numbers. RAE Technical Report to be published
9	L.H. Townend	Ramjet propulsion for hypersonic aircraft. Euromech 3, Supersonic Flow with Heat Addition, February 1966

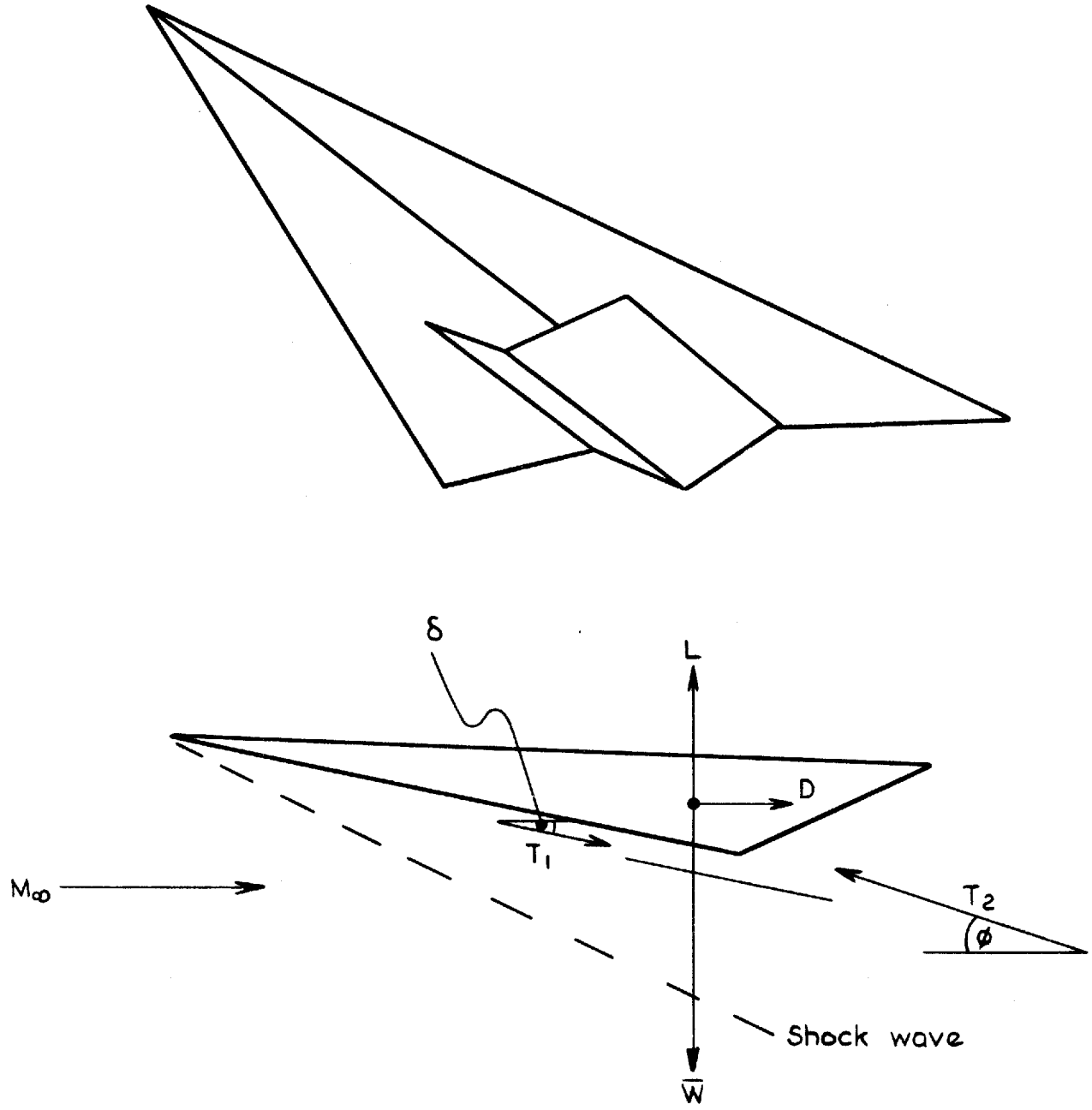

$\bar{W}$ Weight of aircraft in flight

L Lift

D Pressure and friction drag

T_1 Static and momentum pressures integrated over intake entry

T_2 Thrust from nozzle etc (see appendix A)

Fig.1 Schematic diagram of a hypersonic cruise vehicle

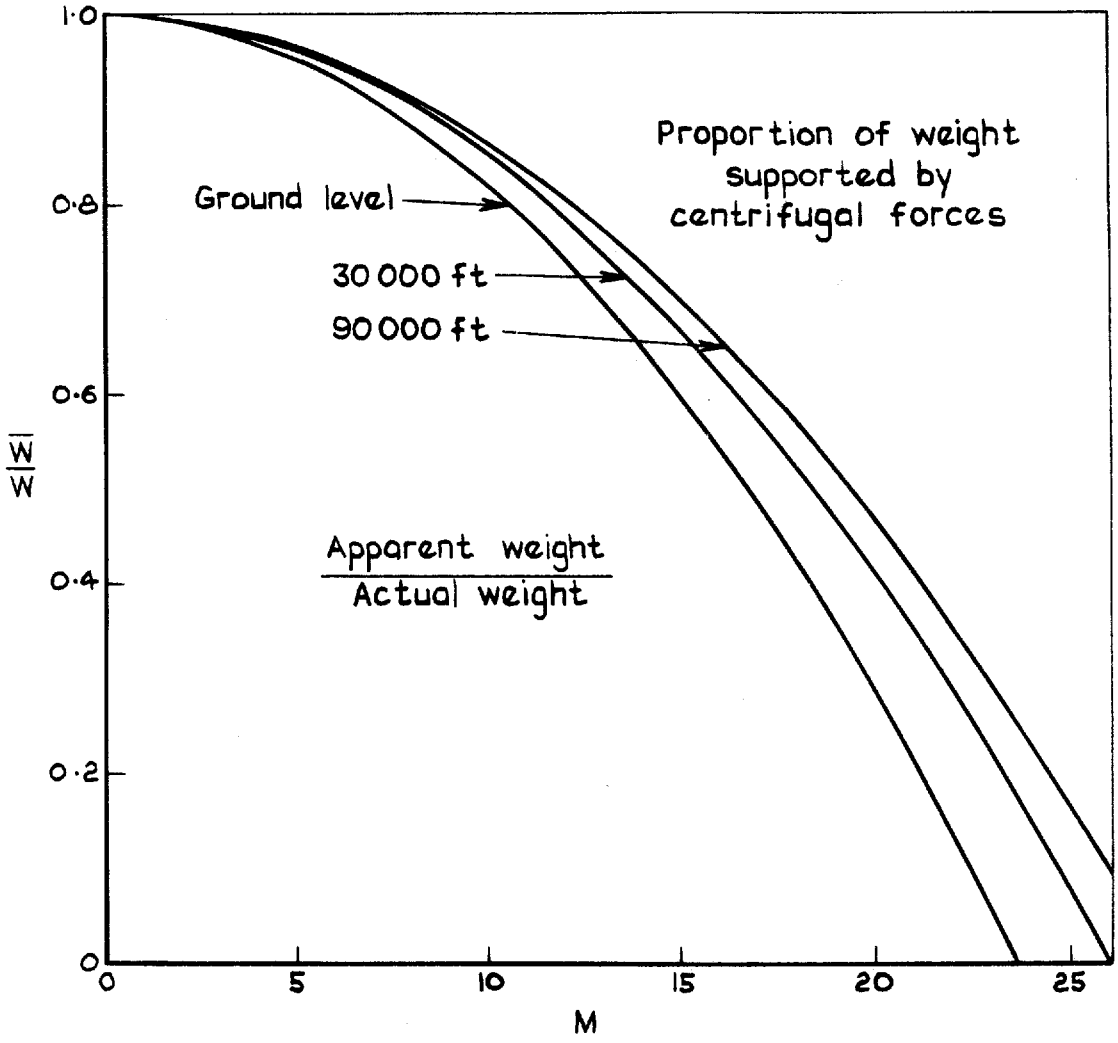

Fig. 2 Influence of centrifugal forces on the apparent weight of an aircraft

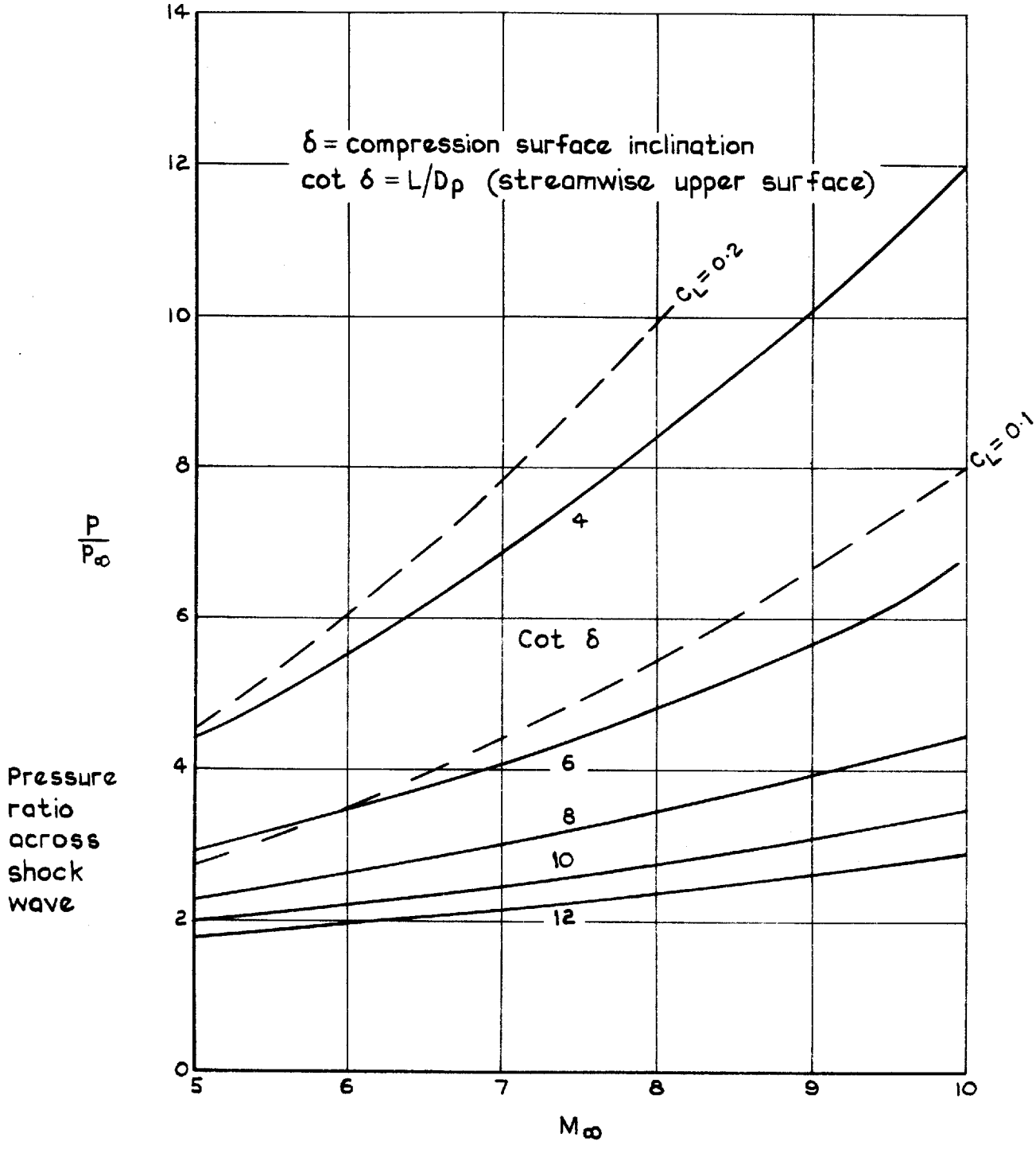

Fig.3 Shock wave compression ratio for caret wings

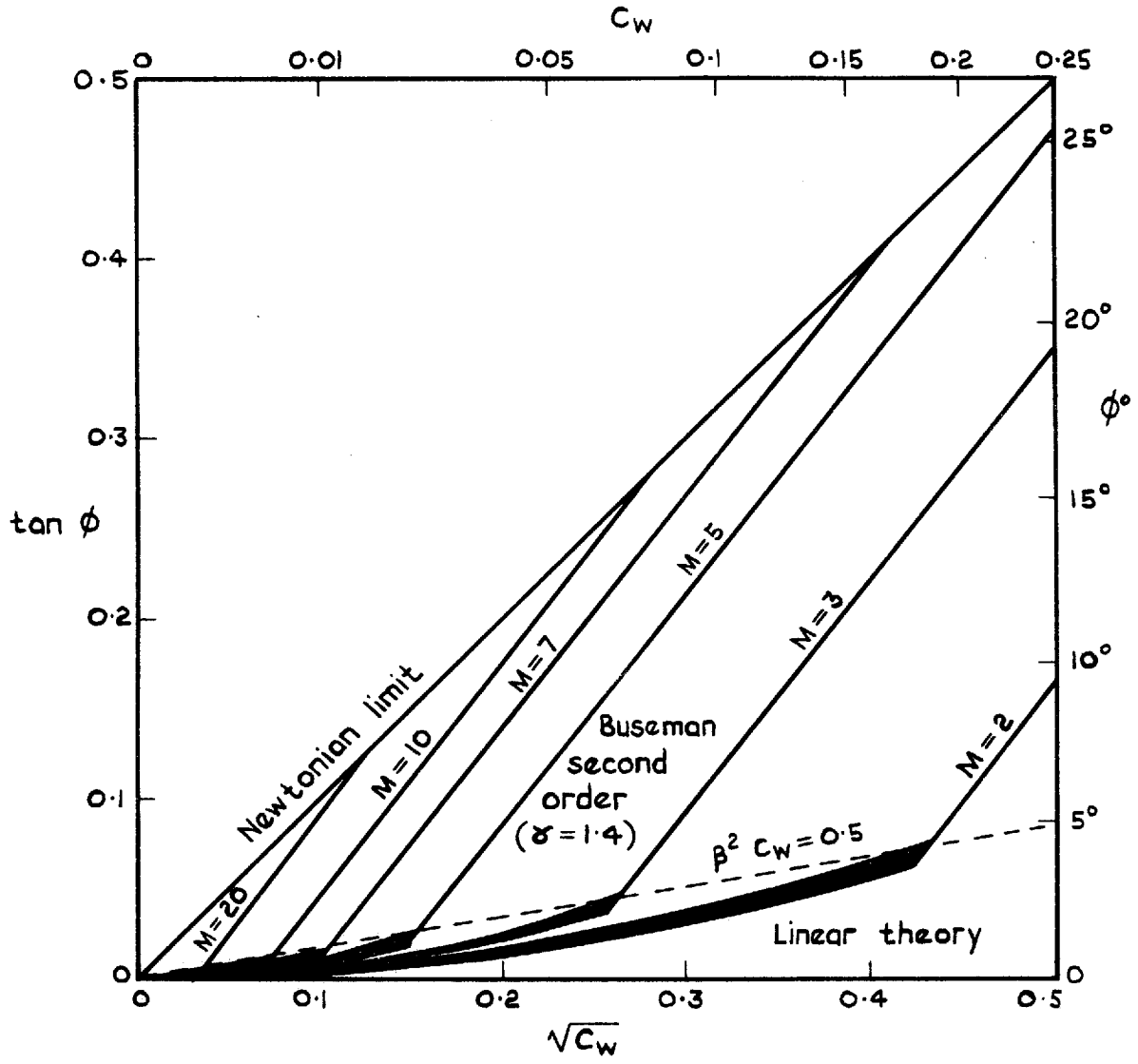

Fig. 4 The optimum nozzle deflection angle ϕ, from three approximate aerodynamic relationships

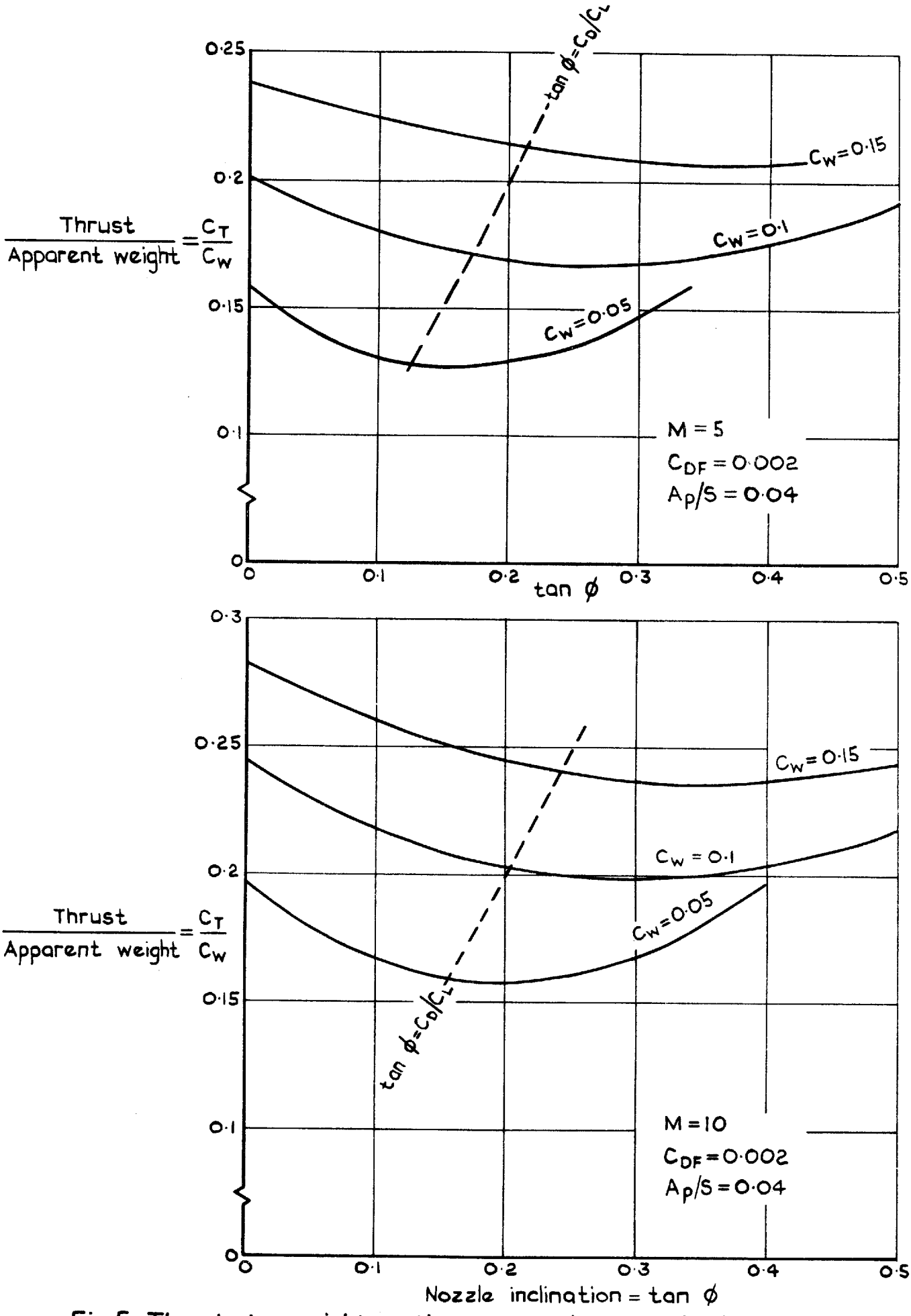

Fig. 5 Thrust to weight ratio for varying nozzle inclination

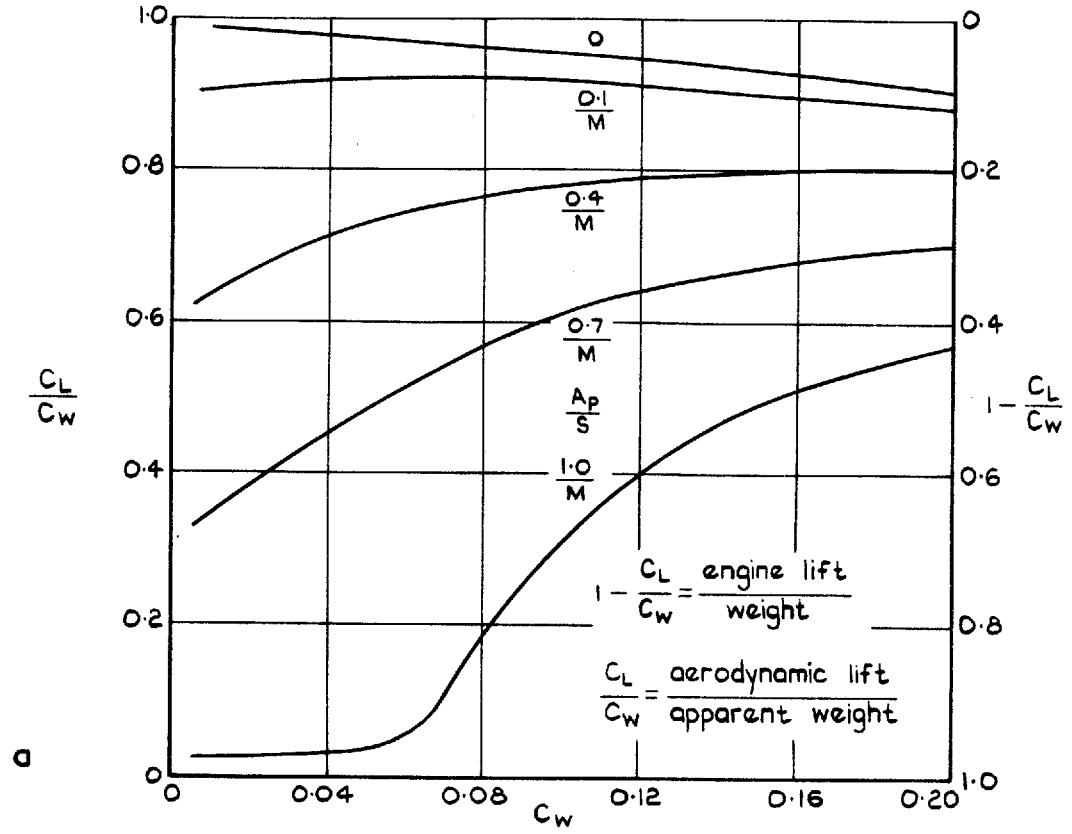

a

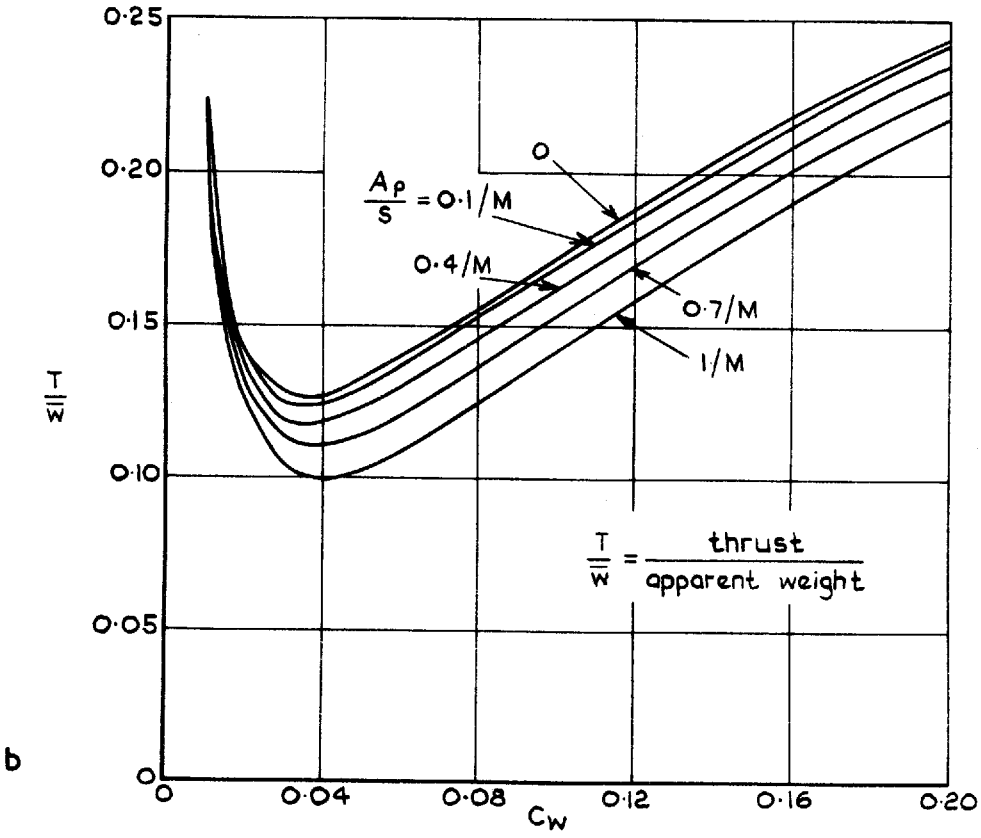

b

Fig. 6 a&b Minimum engine thrust results, M=5, C_{DF}=0·002

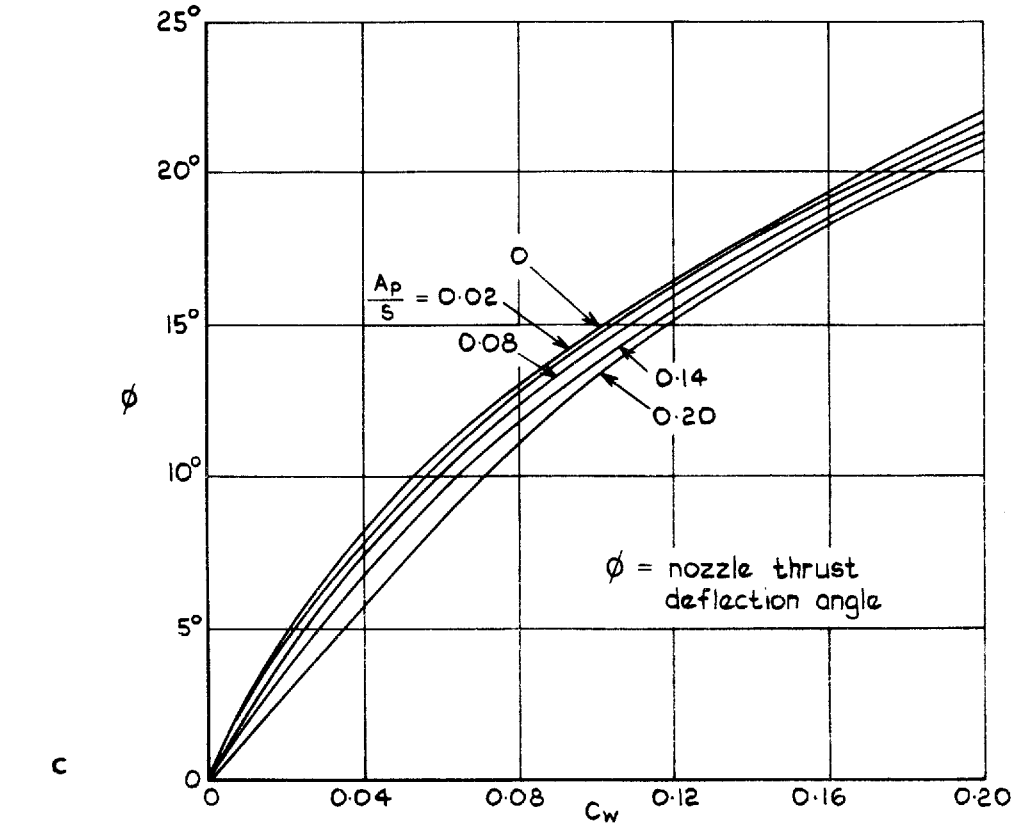
25°
20°
15°
10°
5°
0
ϕ
0
0.04
0.08
0.12
0.16
0.20
Cw
Ap/S = 0.02
0.08
0
0.14
0.20
ϕ = nozzle thrust deflection angle

c

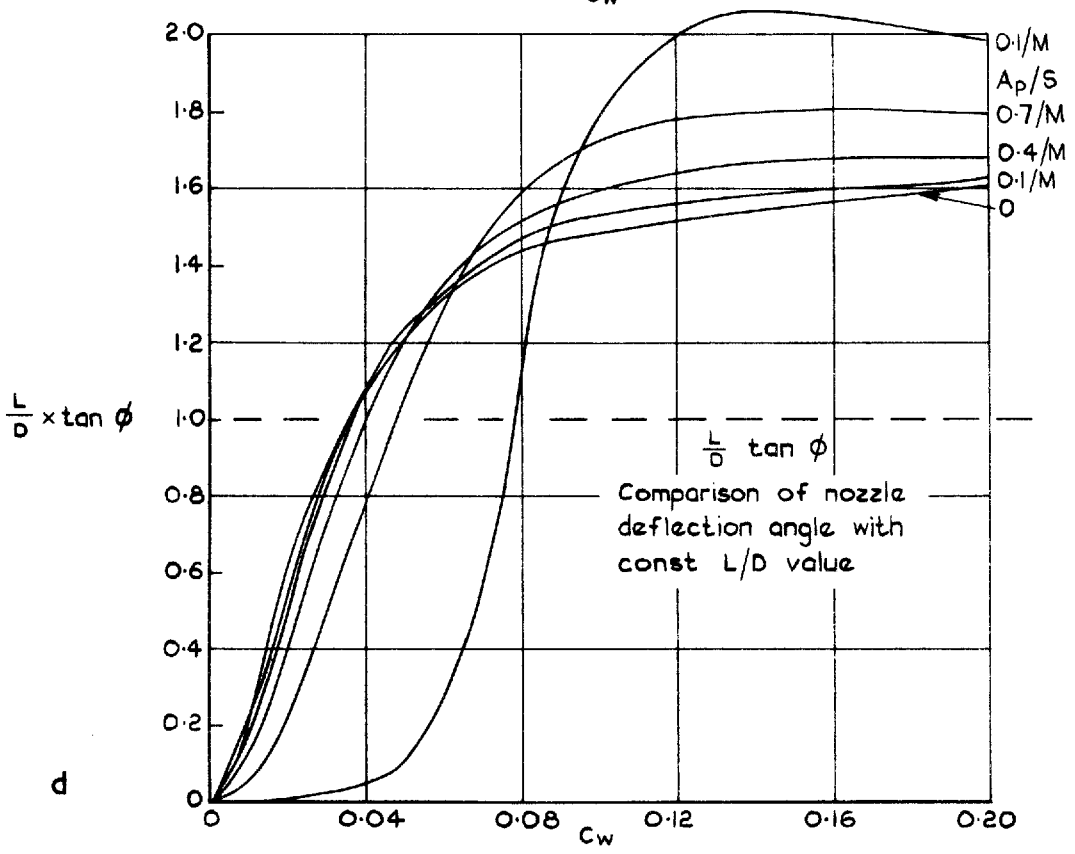
2.0
1.8
1.6
1.4
1.2
1.0
0.8
0.6
0.4
0.2
0
L/D × tan ϕ
0
0.04
0.08
0.12
0.16
0.20
Cw
0.1/M
Ap/S
0.7/M
0.4/M
0.1/M
0
L/D tan ϕ
Comparison of nozzle deflection angle with const L/D value

d

Fig.6 cont

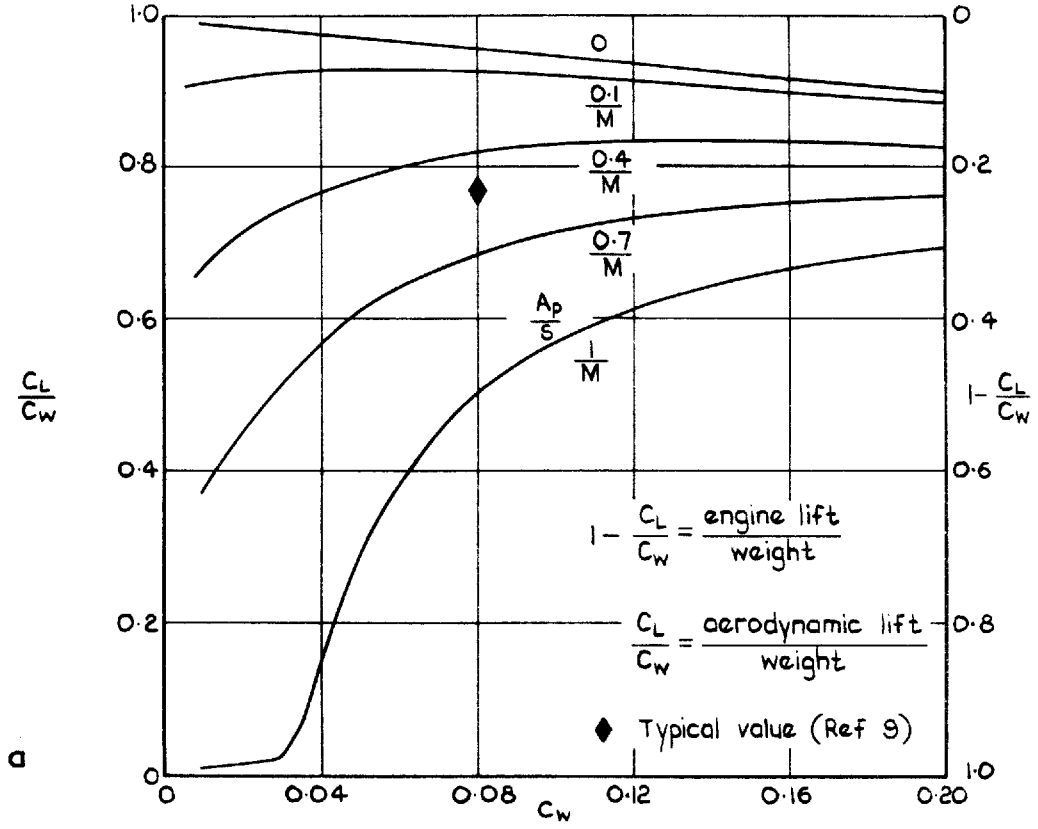

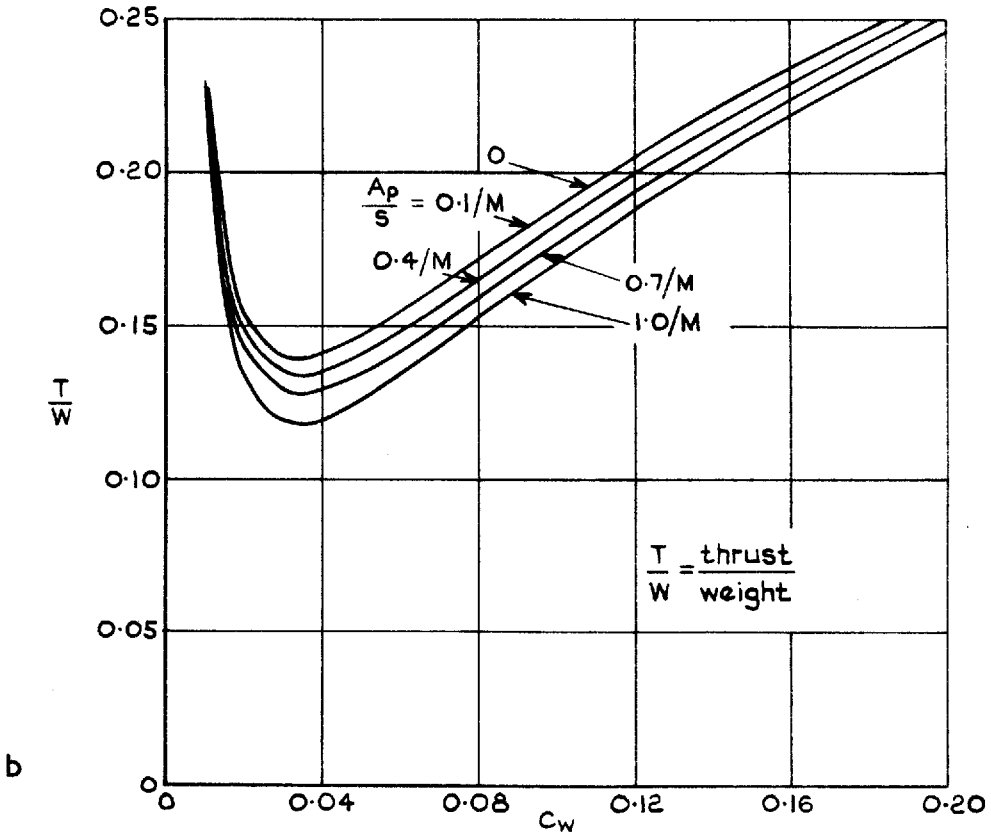

Fig.7 a & b Minimum engine thrust results, for M = 7, C_{DF} = 0·002

c

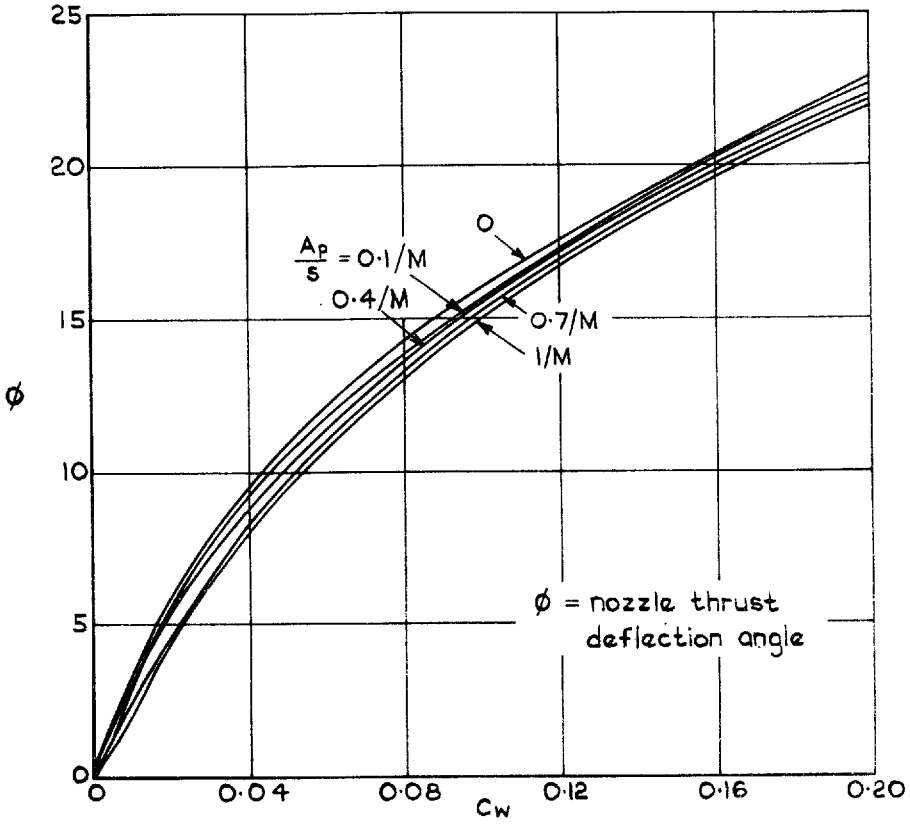
25
20
15
10
5
0
φ
0
0·04
0·08
0·12
0·16
0·20
C_W
$\frac{A_P}{S}$ = 0·1/M
0·4/M
0·7/M
1/M
0
φ = nozzle thrust deflection angle

d

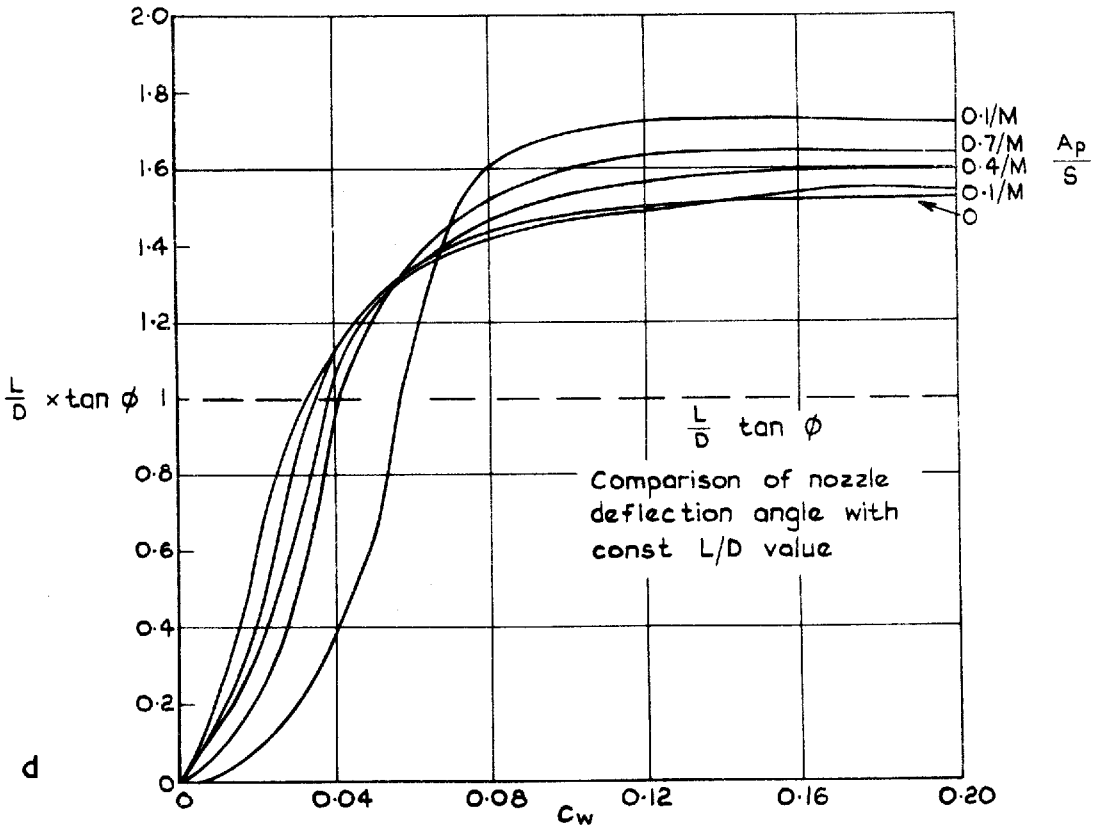
2·0
1·8
1·6
1·4
1·2
1
0·8
0·6
0·4
0·2
0
$\frac{L}{D}$ × tan φ
0
0·04
0·08
0·12
0·16
0·20
C_W
0·1/M
0·7/M
0·4/M
0·1/M
0
$\frac{A_P}{S}$
$\frac{L}{D}$ tan φ
Comparison of nozzle deflection angle with const L/D value

Fig. 7 cont

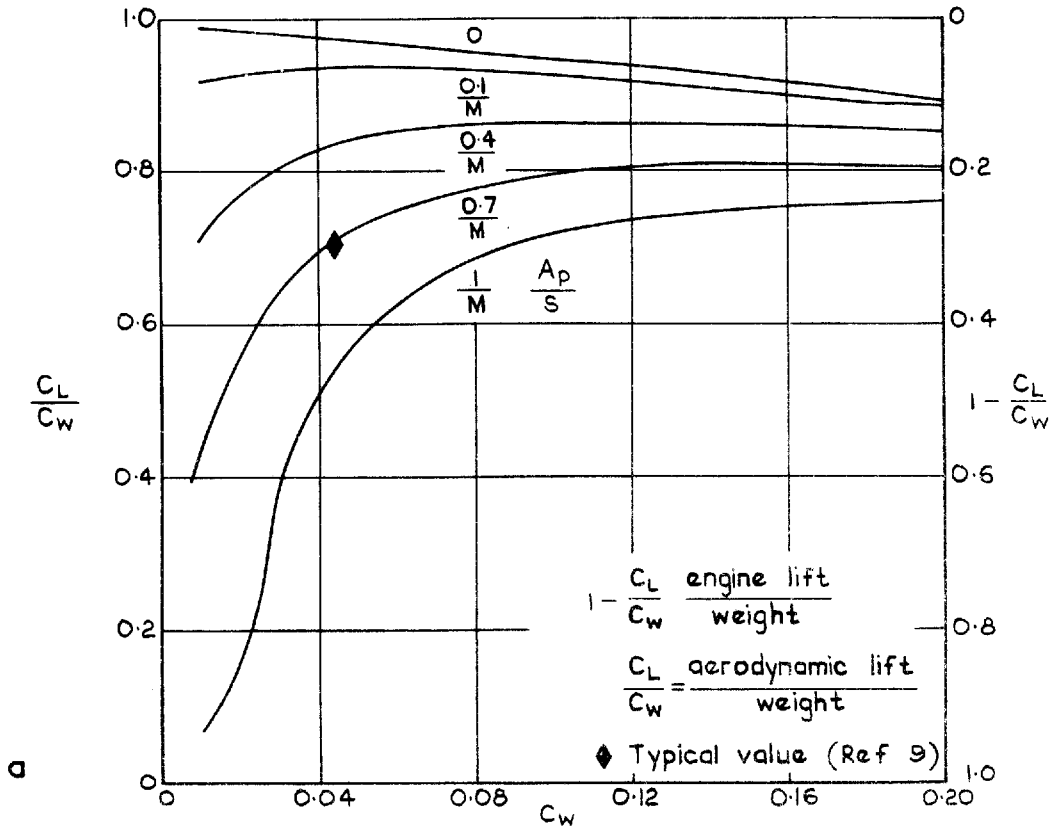

a

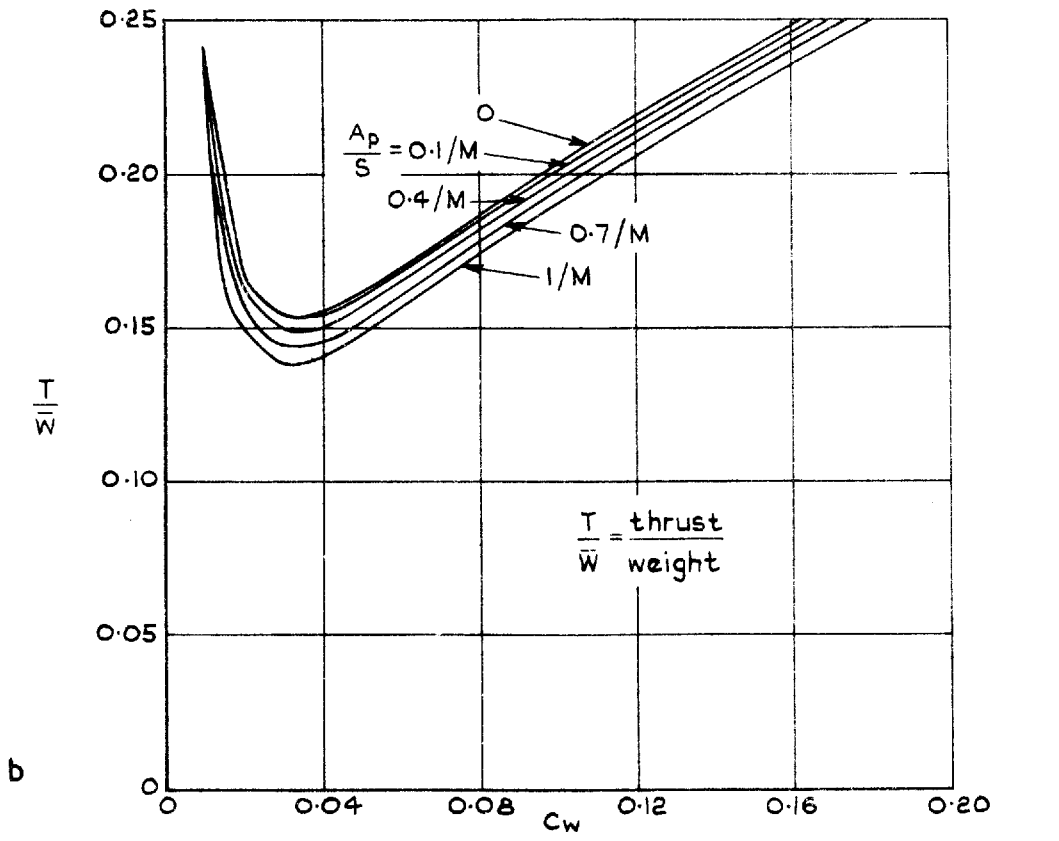

b

Fig. 8 a&b Minimum engine thrust results, M = 10, C_{DF} = 0·002

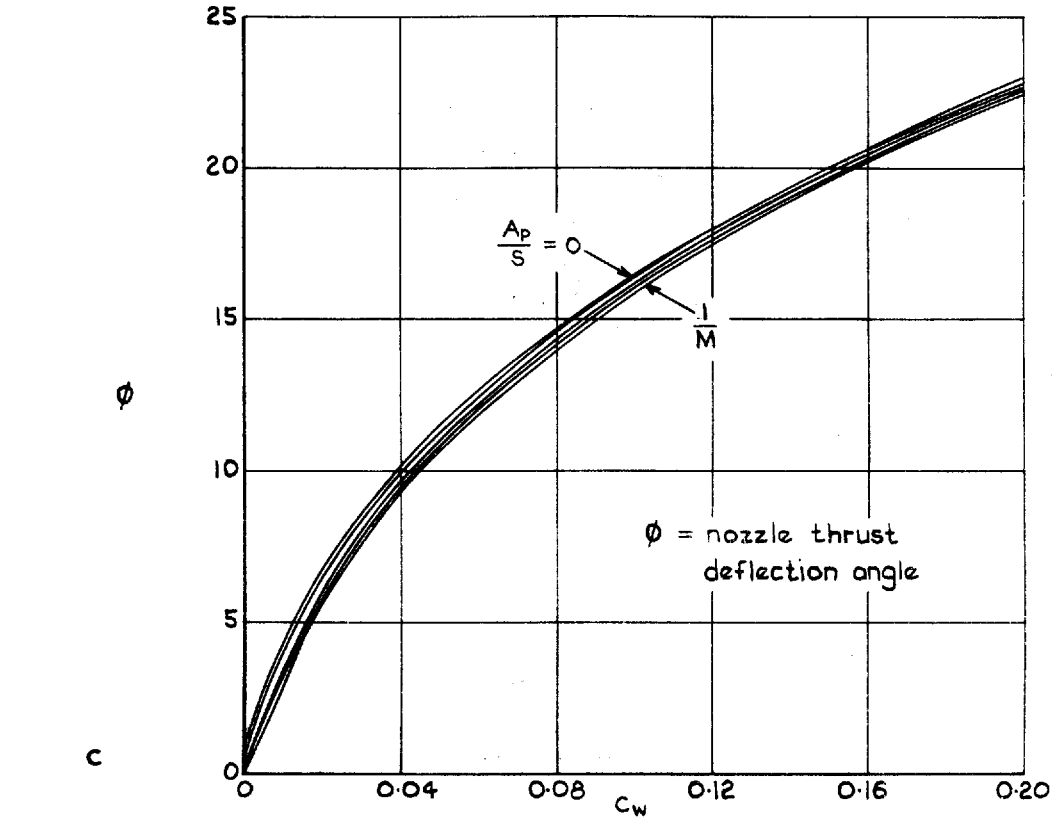
25
20
15
10
5
0
φ
$\frac{A_p}{S}$ = 0
$\frac{1}{M}$
φ = nozzle thrust deflection angle
0
0·04
0·08
0·12
0·16
0·20
C_w

c

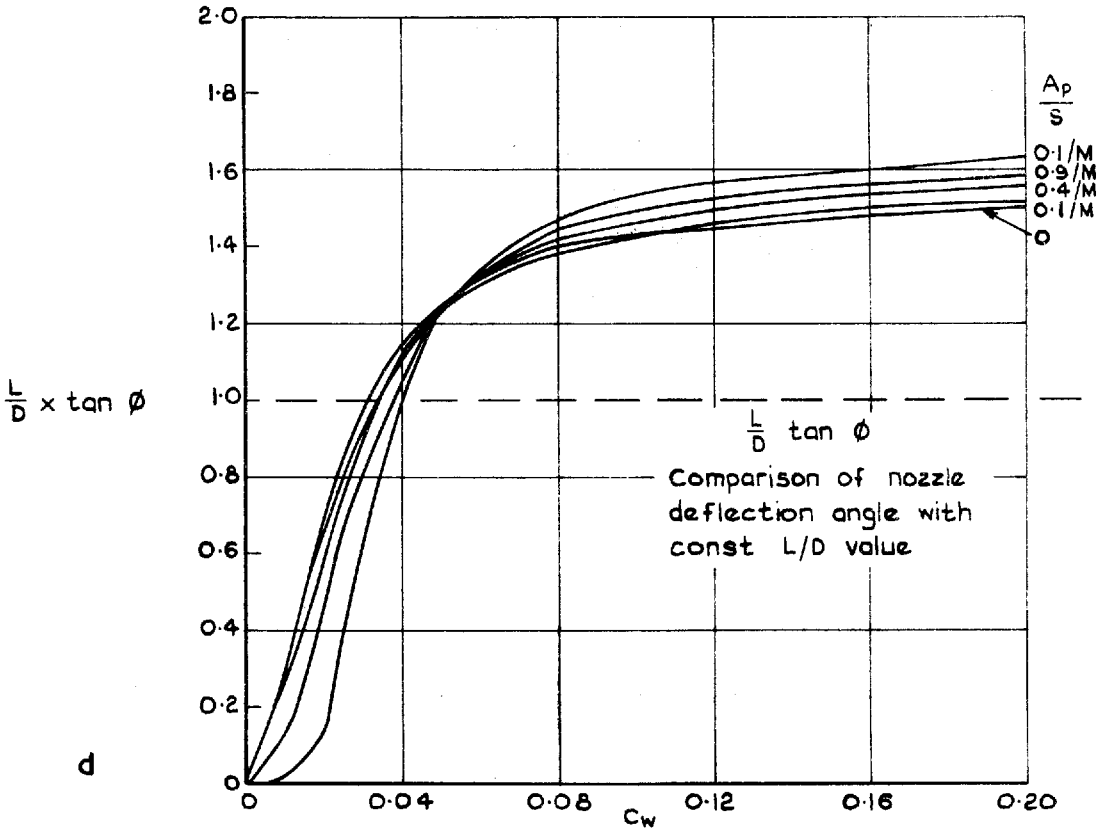
2·0
1·8
1·6
1·4
1·2
1·0
0·8
0·6
0·4
0·2
0
$\frac{L}{D}$ x tan φ
$\frac{A_p}{S}$
0·1/M
0·9/M
0·4/M
0·1/M
0
$\frac{L}{D}$ tan φ
Comparison of nozzle deflection angle with const L/D value
0
0·04
0·08
0·12
0·16
0·20
C_w

d

Fig. 8 cont

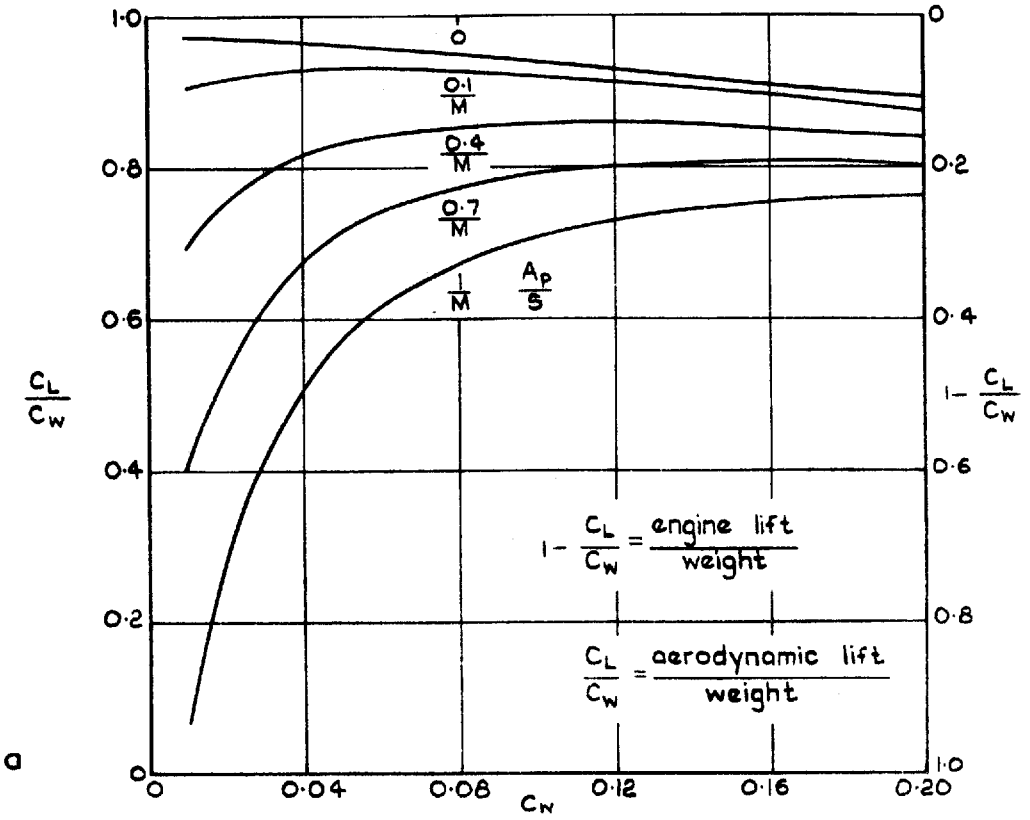

a

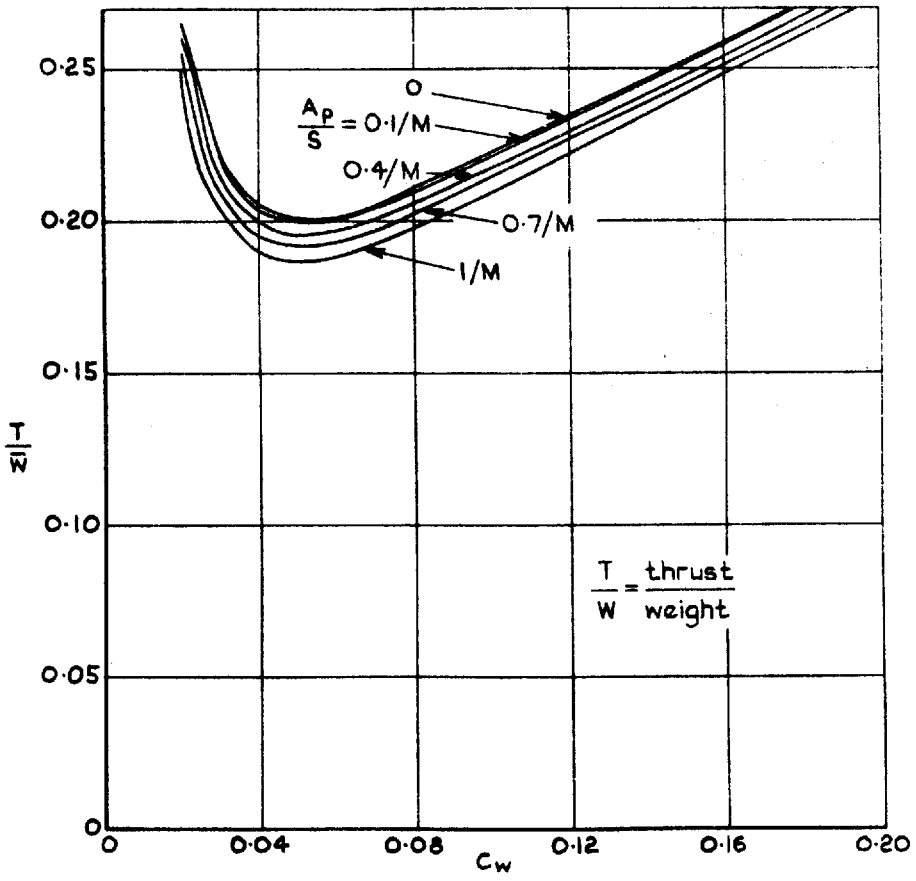

b

Fig.9 a&b Minimum engine thrust results, for large friction drag M=10, $C_{DF}=0·004$

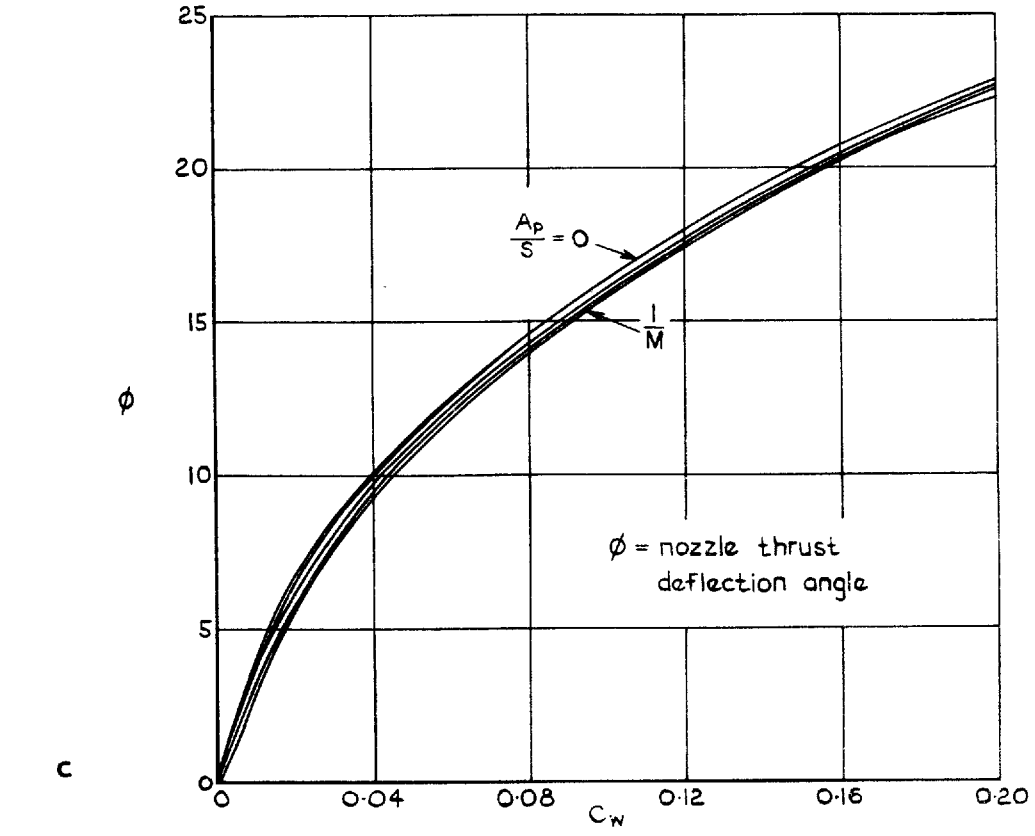
25
20
15
10
5
0
φ
$\frac{A_p}{S} = 0$
$\frac{1}{M}$
φ = nozzle thrust deflection angle
0
0·04
0·08
0·12
0·16
0·20
C_w

c

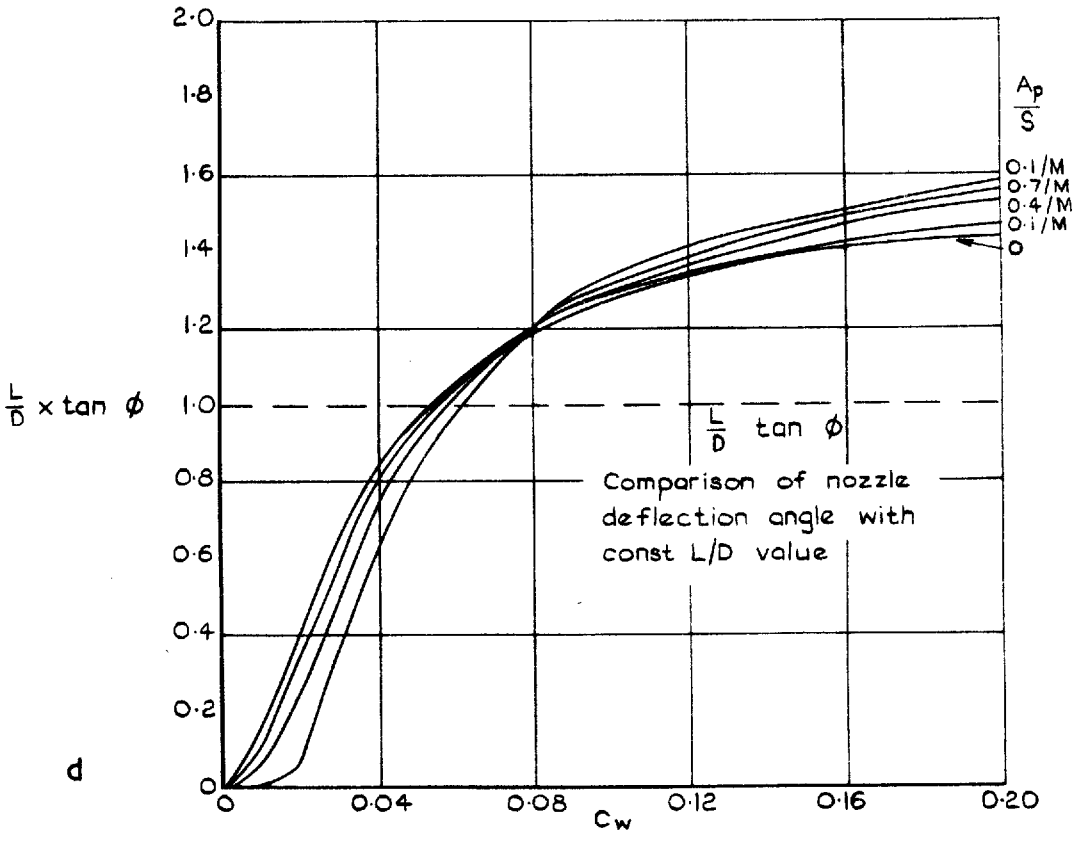
2·0
1·8
1·6
1·4
1·2
1·0
0·8
0·6
0·4
0·2
0
$\frac{L}{D} \times \tan \phi$
$\frac{A_p}{S}$
0·1/M
0·7/M
0·4/M
0·1/M
0
$\frac{L}{D} \tan \phi$
Comparison of nozzle deflection angle with const L/D value
0
0·04
0·08
0·12
0·16
0·20
C_w

d

Fig. 9 cont

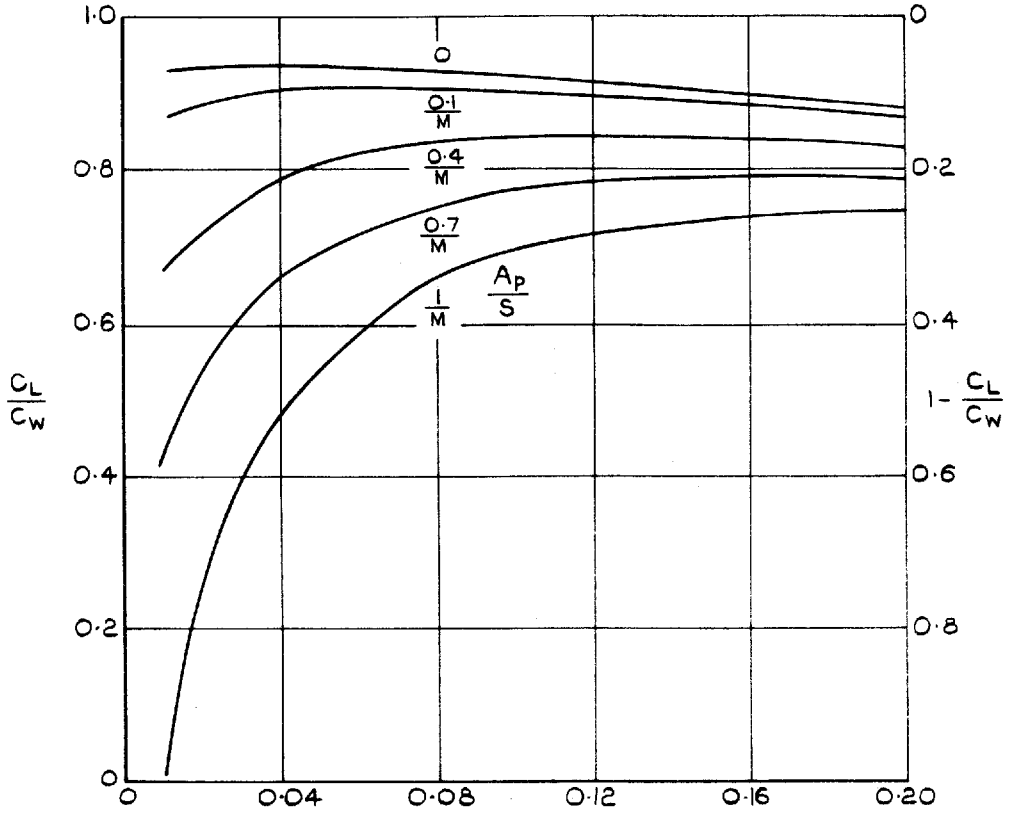

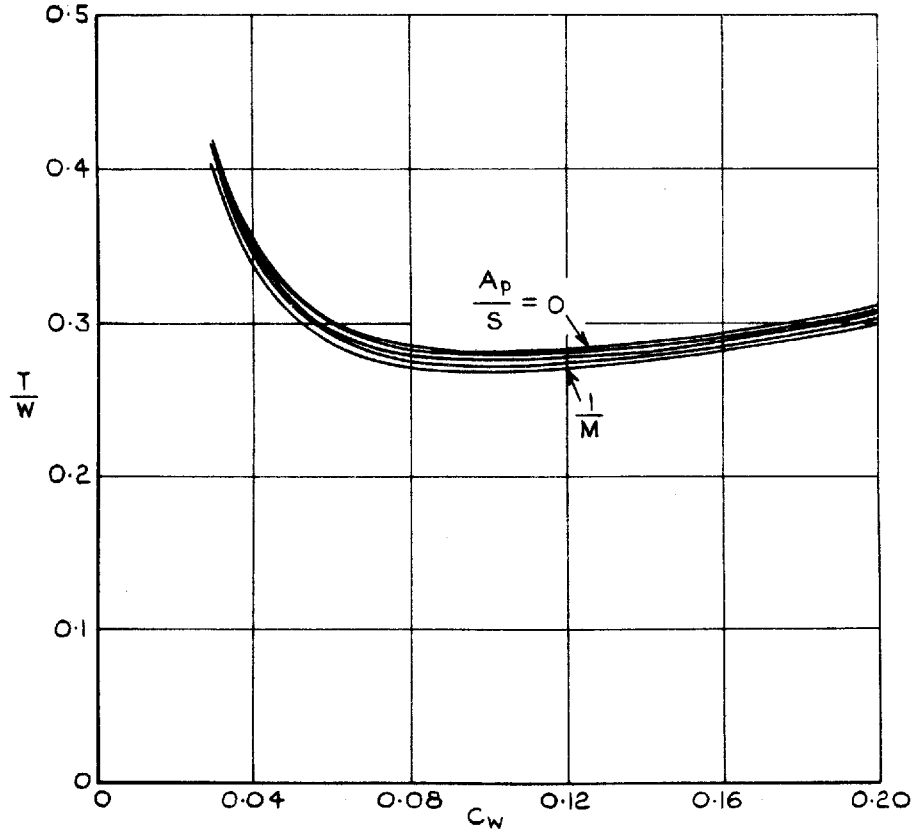

Fig.10a&b Minimum engine thrust results, for very large friction drag $M = 10$, $C_{DF} = 0{\cdot}01$

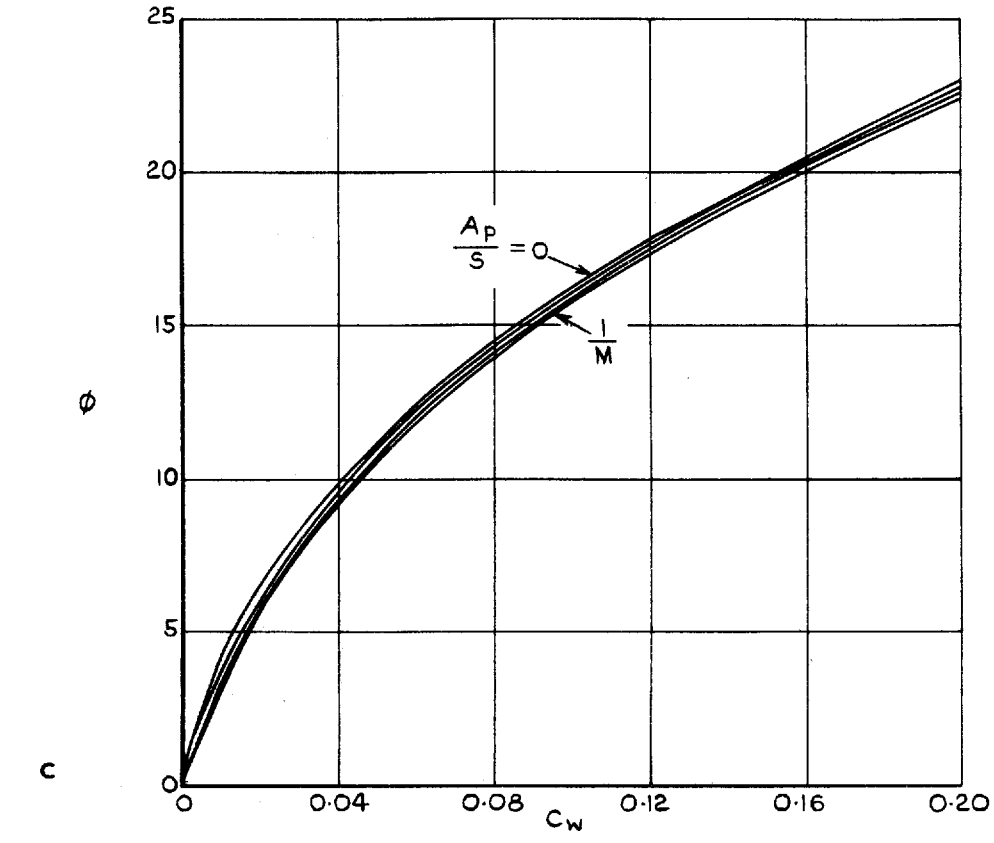

c

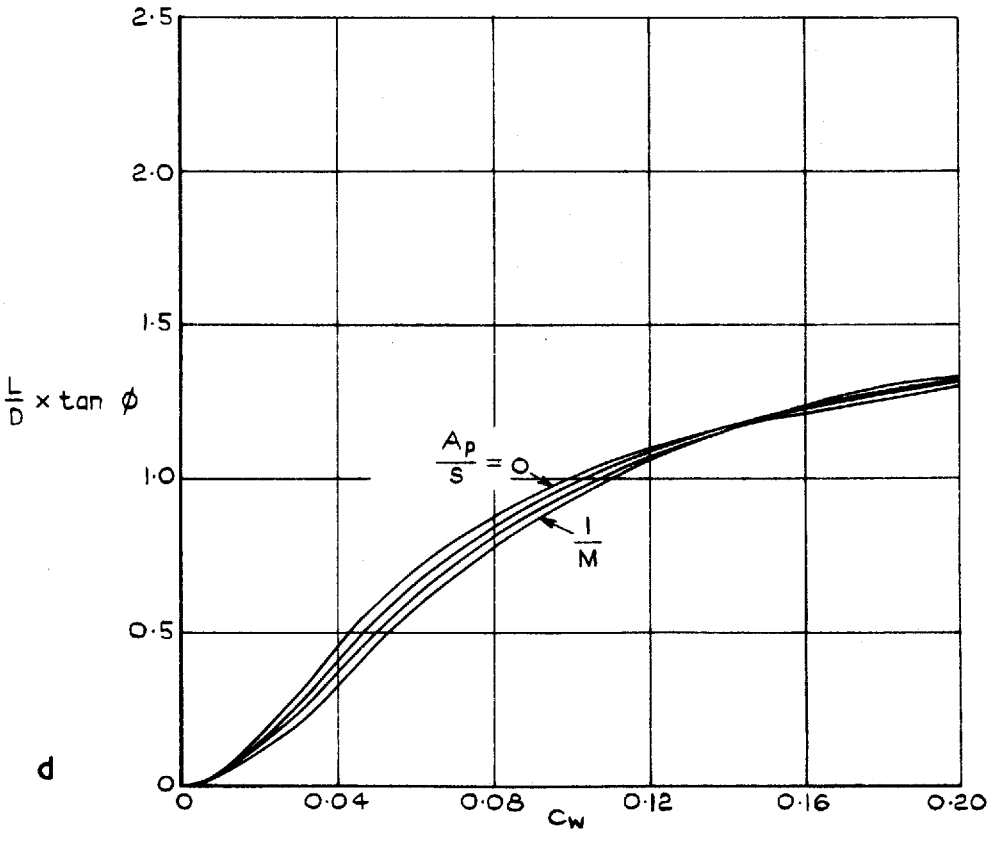

d

Fig. 10 cont

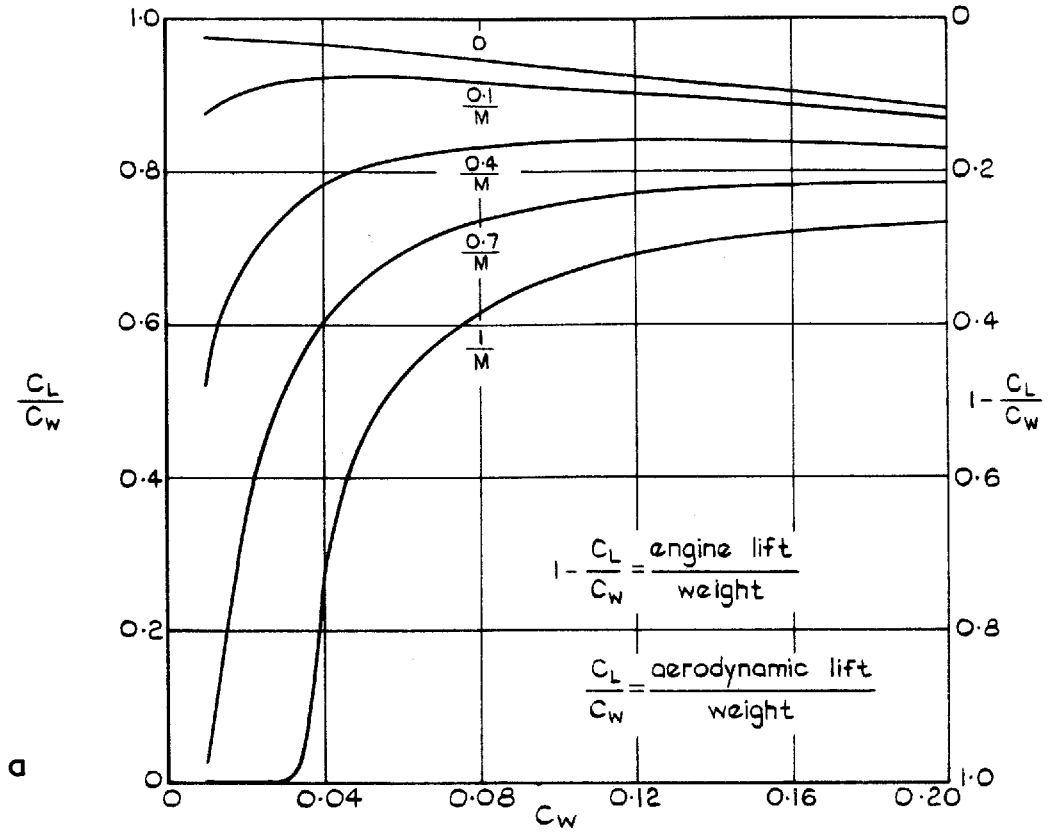

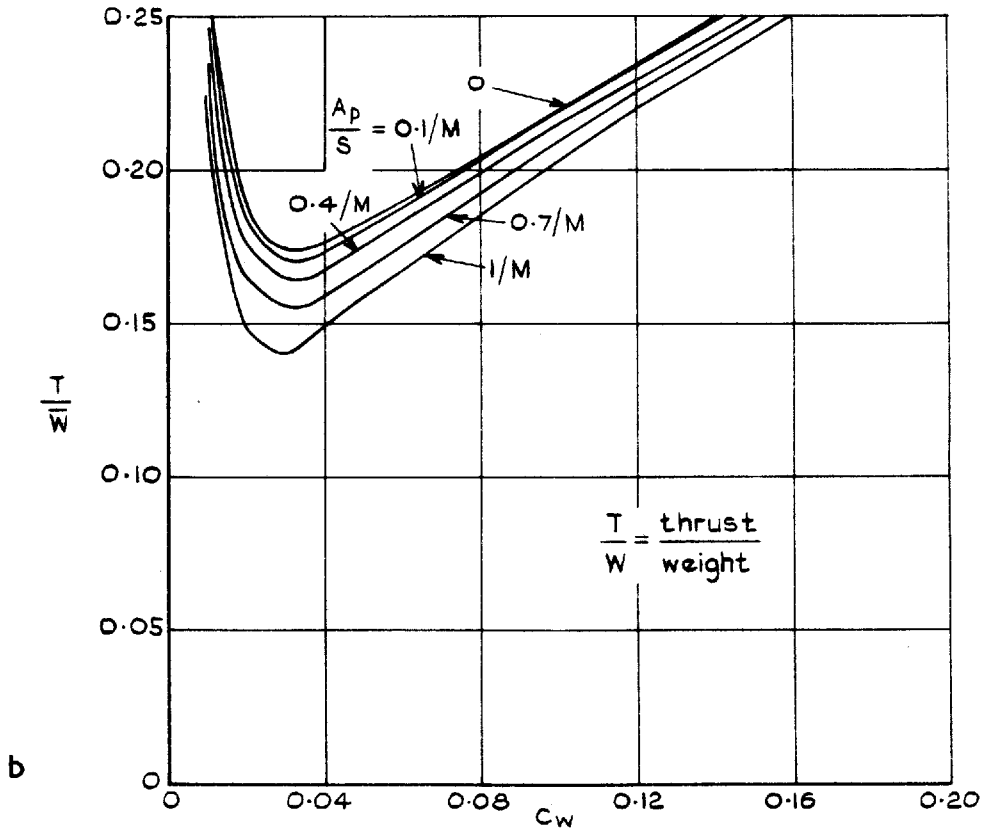

Fig. 11a&b Minimum engine thrust results, for friction drag varying with C_L, $M=10$, $C_{DF}=0·002\,(1+10\,C_L)$

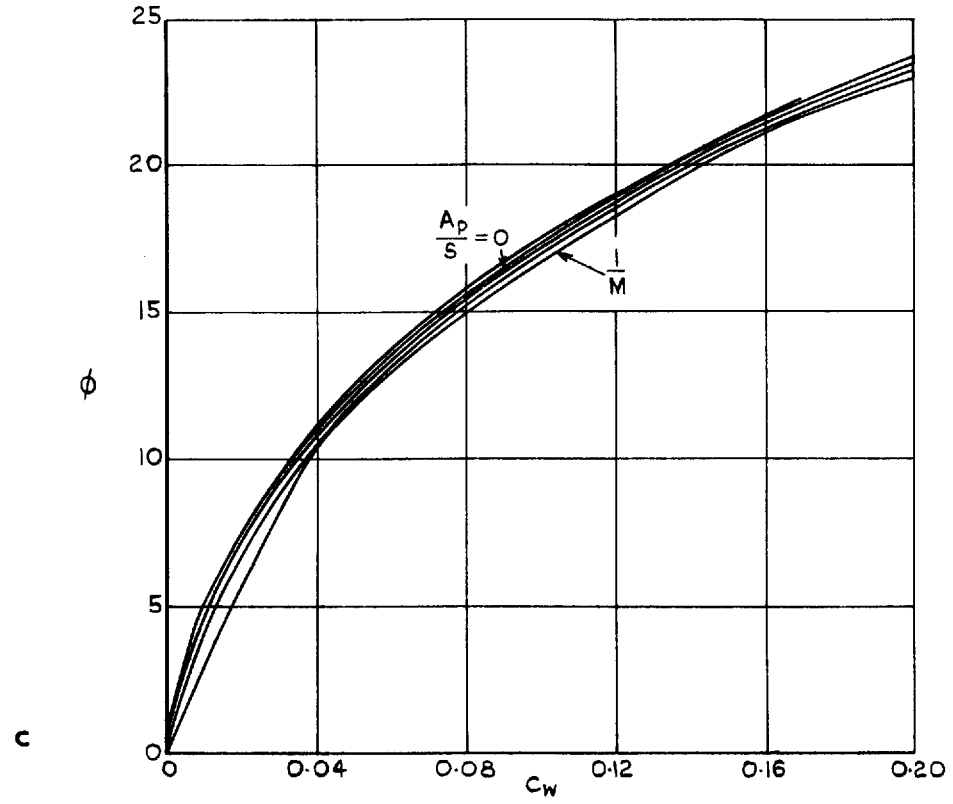

c

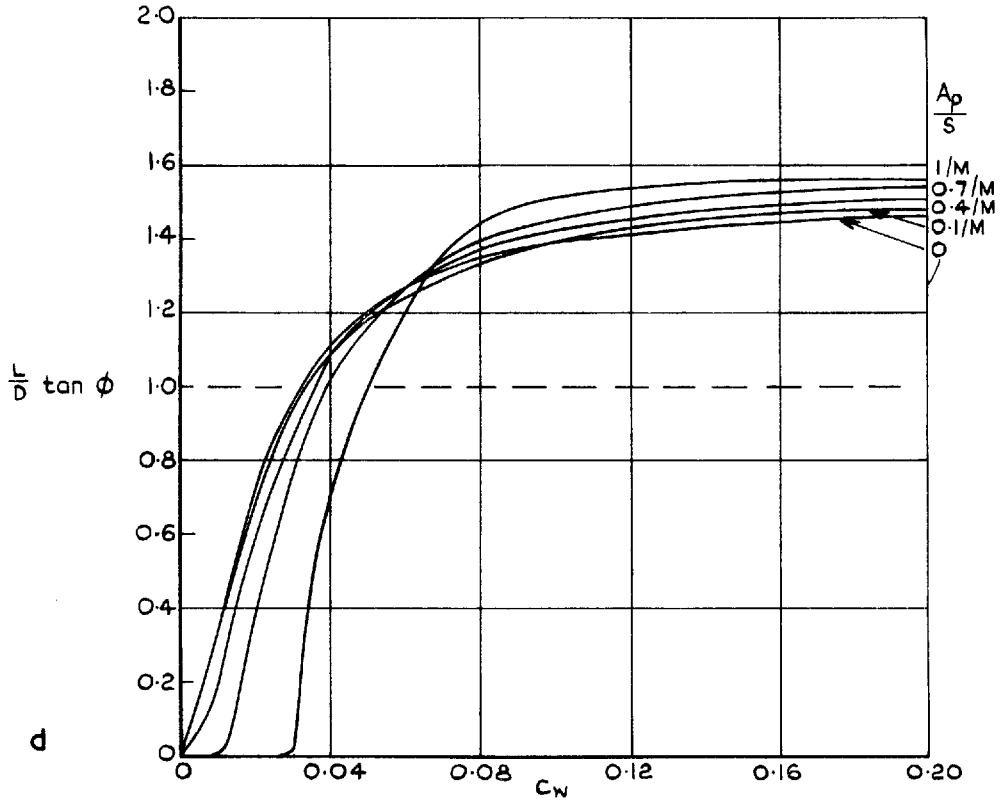

d

Fig.11 cont

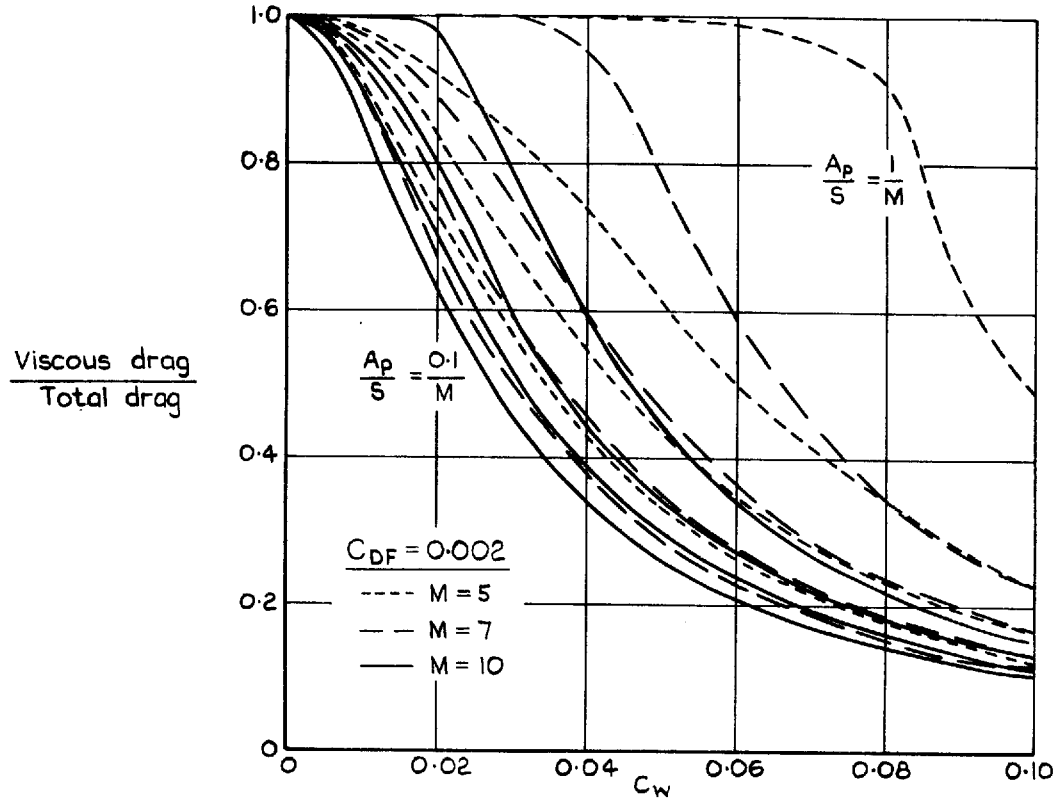

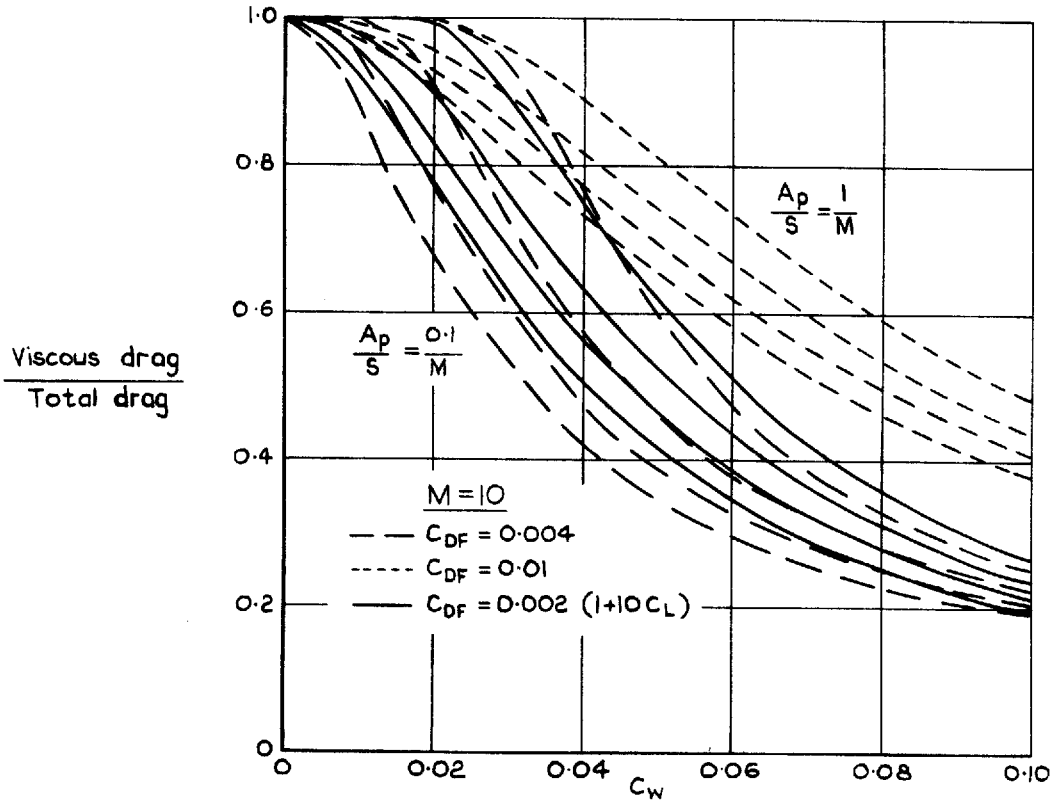

Fig.12 Ratio of viscous drag to total drag

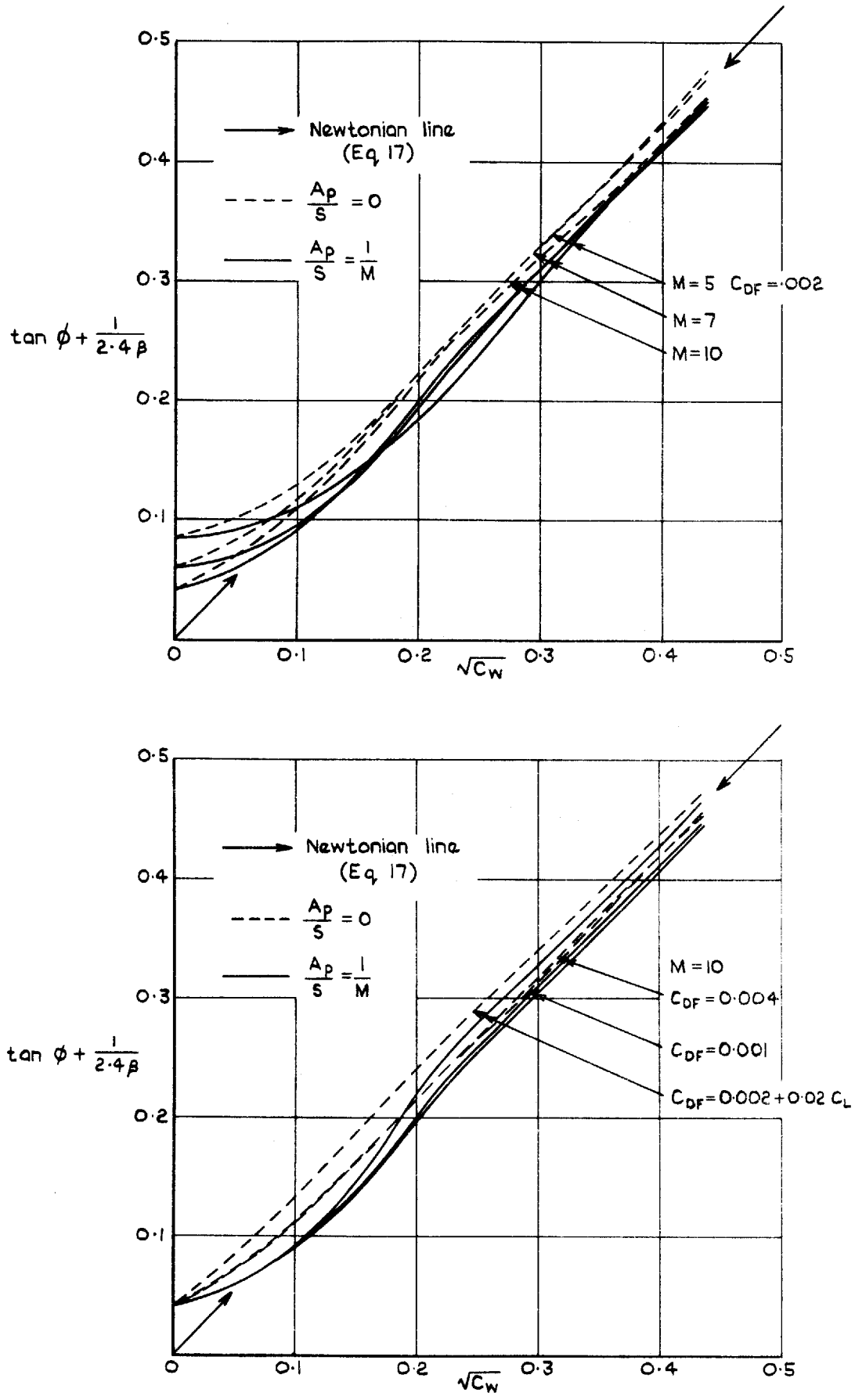

Fig. 13 Collapsed plots of ϕ values

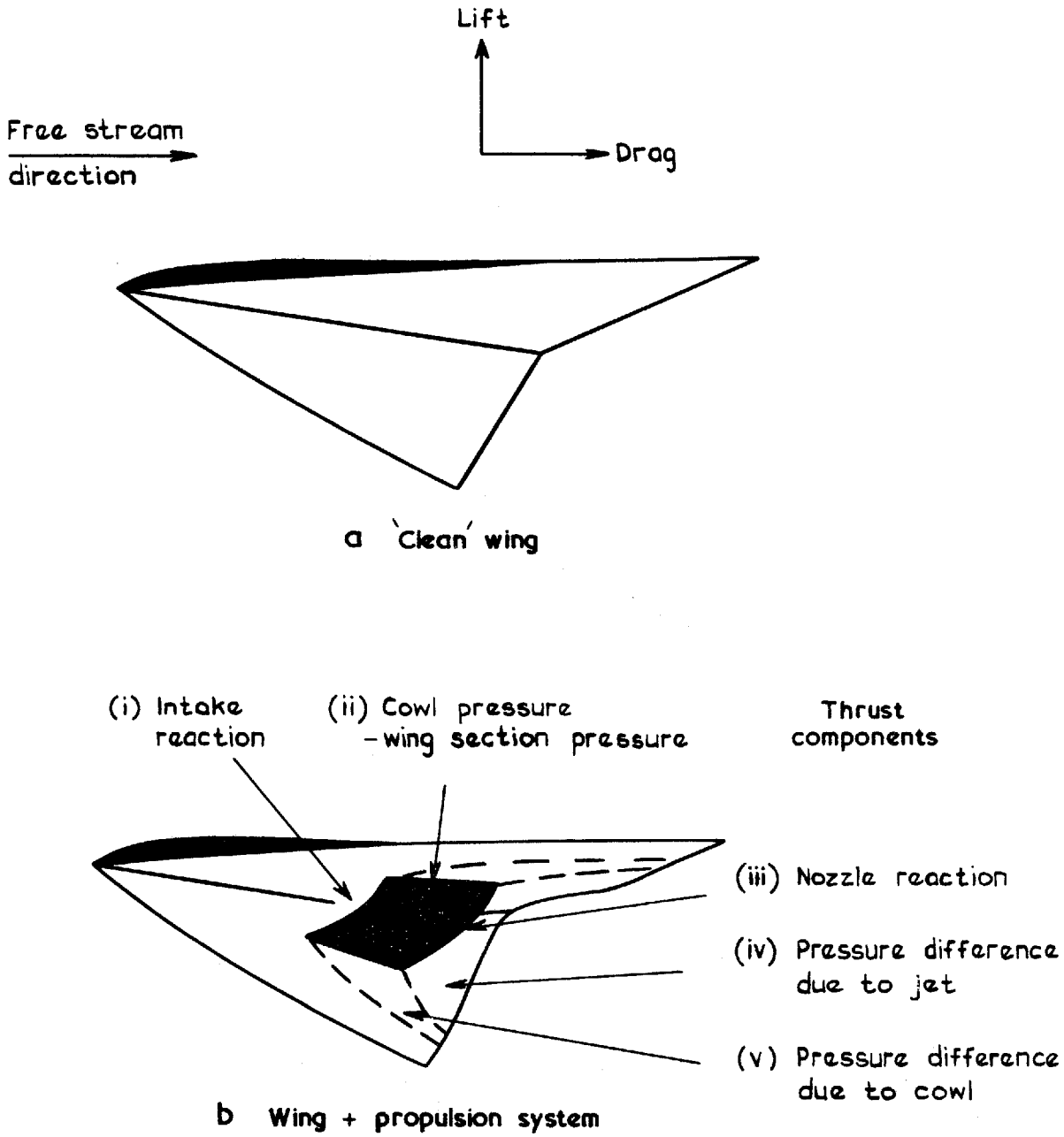

Fig. 14a-c Schematic representation of a lifting configuration with and without propulsion unit

Printed in England for Her Majesty's Stationery Office by the Royal Aircraft Establishment, Farnborough. Dd.503427. K.4.